Soil Moisture Dynamics in Urban Areas

Identifying the relationship between soil moisture content and drought in urban areas

M.S.J. van Zon

Technische Universiteit Delft

Soil Moisture Dynamics in Urban Areas

Identifying the relationship between soil moisture content and drought in urban areas

by

M.S.J. van Zon

to obtain the degree of Master of Science

at the Delft University of Technology,

Student number:	4699572	
Project duration:	July, 2024 – March 2025	
Thesis committee:	Dr. ir. A.M.J. Coenders,	TU Delft, supervisor
	Dr. ir. J.A. van der Werf,	TU Delft
	Dr. ir. J. Langeveld,	TU Delft
	ir. B.H. van der Scheer,	SWECO

Acknowledgement

This master's thesis marks the end of my time as a student in Delft. Over the past eight years, both the city and the university have become like home to me. Throughout this master's, I've learned a great deal about what I am passionate about and the field I feel like ready to pursue in my career, now that my master's is complete. This final project has been crucial in finishing my master's, and I could not have done it alone. The discussions with friends, supervisors, and many others were vital in allowing me to finish this work. Therefore, I would like to take this opportunity to express my gratitude to them.

First of all, I would like to express my gratitude to my thesis committee. A special thank you to my daily supervisors, Miriam and Job, for your guidance in quickly setting up my thesis and enabling me to capture the summer of 2024. I am grateful for the guidance throughout the process, as well as your invaluable feedback and the encouragement to stay on track when I was lost in my own research. Thank you Jeroen, for being the external supervisor and providing critical feedback to my research. Together, you all sparked my enthusiasm for this topic, which I initially thought wasn't as interesting as some of the other subjects within the master's program. From Sweco, I would like to thank Bor for your guidance throughout the project. You always made time for me and provided valuable motivation, offering insights from your company's perspective. Your viewpoint on my research from a business standpoint was particularly helpful and gave me a broader understanding of my work.

Beyond my committee, my thesis would not have been possible without Thom, who assisted me with setting up my data collection, provided all the required equipment, and helped me with the measurement procedures and model discussions. I am also grateful to CREFM for the opportunity to conduct my experiments at the TU Delft campus.

Finally, I would like to thank my friends and family who supported me during my thesis and the eight years before. Mats and Floris, thank you for continuing my measurements while I was on holiday; without you, my dataset wouldn't be as extensive as it is now. A big thank you to all my friends in Delft, who have been there to listen to me and share unforgettable memories and adventures. Thank you to the people from the Afstudeerhok whom I have spent most hours with working on my thesis. I am also grateful to my parents, little brother and sister, who encouraged me to follow my passion and supported me every step of the way, to celebrate the highs and help me through the lows. Lastly, a heartfelt thank you to my boyfriend for always being there when needed, through both the good times and the challenges. I am truly grateful for the opportunity to have had such an amazing experience as a student in Delft, and I can't wait to see what comes next!

Enjoy reading!

M.S.J. van Zon
Delft, March 2025

Summary

Climate change poses increasing challenges to urban environments, with rising temperatures, sea-level rise, and altered precipitation patterns contributing to both flooding and drought. While much research has been dedicated to flood mitigation, urban drought has received comparatively less attention, despite its significant impact on vegetation, water availability, and overall ecosystem stability. The Paris Agreement of 2016 aims to limit global temperature increases, yet urban areas continue to experience extreme weather variations, necessitating a deeper understanding of their hydrological implications.

This thesis investigated the influence of urban environmental conditions on soil moisture dynamics, particularly during drought periods. The study aims to identify the relationship between green spaces in urban areas and soil moisture dynamics in relation to drought. It specifically examines how factors such as sun, shadow, vegetation type, and soil texture impact soil moisture retention and depletion. To achieve this research goal, the following three research questions are determined:

1. How do urban environmental conditions affect soil moisture content in green spaces?
2. What is the effect of soil texture on soil moisture dynamics?
3. How do initial soil moisture conditions influence soil moisture dynamics during a drought period, as modelled using HYDRUS-1D?

The study employs a combination of field measurements and HYDRUS-1D modelling, to analyse the soil moisture behaviour under different urban environmental conditions. Data collection took place at the campus of Delft University of Technology, where five distinct environmental conditions were selected as measurement points, sun, shadow, grass, trees and paved areas.

Soil moisture data was collected using the Profile Probe PR1 sensor (in combination with the HH2 Moisture Meter) at depths of 100mm, 200mm, 300mm, 600mm and 1000mm. Measurements were conducted manually over 10 weeks, 3 to 4 times a week, during the summer of 2024, with a total of 33 recorded sessions. Soil texture analysis was conducted using soil samples taken from depths of 150mm, 300mm, 500mm and 800mm. These samples were dried at 105°C for 24 hours and then sieved through six mesh sizes to determine the proportion of sand, silt and clay in each sample. The soil texture provided understanding of changes in soil moisture dynamics and was used for the critical input data for the HYDRUS-1D simulations.

HYDRUS-1D was employed to model the impact of initial soil moisture conditions and urban environmental conditions on the soil moisture dynamics during longer periods of drought. The model setup included defining soil hydraulic properties using the van Genuchten-Mualem equation and incorporating root water uptake parameters based on the Feddes approach. Monte Carlo simulations were conducted to optimize model performance, using 10.000 iterations to determine the best fitting parameters. The model was then applied to simulate soil moisture depletion during the extreme drought of 2018, to determine the effects of extremely wet or dry initial soil moisture conditions.

The measured soil moisture content results demonstrate significant variations in soil moisture retention among different urban environment conditions. Areas covered with vegetation exhibited higher moisture retention compared to paved surfaces. Within vegetated areas, shaded locations retained moisture for longer periods due to reduced evaporation rates. In contrast, measurement points in sunny areas experienced rapid soil moisture depletion, particularly in the upper 300mm of the soil.

Soil moisture at shallower depths, 100mm to 300mm, was highly responsive to precipitation events, while the deeper layers, 600mm and 1000mm, exhibited more stable moisture levels, indicating a stronger influence of soil texture and groundwater interactions. Statistical analysis using Kendall's and Spearman's correlation coefficients showed strong correlations between shaded grass-covered areas and tree-covered sites up to 300mm depth, but significant divergence beyond that, likely due to differences in root water uptake and soil texture.

Additionally, paved areas consistently maintained lower soil moisture levels across all depths due to limited infiltration, with only minor variations observed at the access tube edges where small gaps allowed some water entry. The modeling results confirmed that urban design choices, such as increasing permeable surfaces and optimizing vegetation placement, can significantly enhance urban resilience to drought.

Soil texture played a crucial role in soil moisture availability, with finer-textured soils (such as silt and clay) demonstrating superior retention capabilities compared to sandy soils, which facilitated rapid drainage.

Modeling results from HYDRUS-1D reinforced these findings, showing that initial soil moisture conditions had a notable influence on drought resilience. Wetter initial conditions resulted in prolonged moisture availability, while extremely dry conditions led to rapid soil desiccation. The impact of extreme initial soil moisture states was most pronounced in shaded grass areas and tree-covered locations, where higher retention capacity helped delay drought effects.

The study's findings align with existing literature on urban drought dynamics, confirming that meteorological, agricultural and hydrological drought factors interact to shape soil moisture behaviour. Meteorological drought, characterized by prolonged low precipitation, was found to be a primary driver of soil moisture deficits, with its effects compounded by urban environmental conditions. The research underscores the critical role of green infrastructure in mitigating the adverse effects of drought by preserving soil moisture.

The limitations of the study are acknowledged, including the constraints of the HYDRUS-1D model, which assumes only vertical water flow and does not account for lateral redistribution. Additionally, the generic settings of the Profile Probe PR1 resulted in soil moisture values not specifically related to the soil type. Finally, only one drought event has been evaluated in the model, limiting the generalizability of the findings.

This research provides valuable insight into the interplay between urban environmental conditions and soil moisture dynamics during drought periods. The findings highlight the importance of green spaces in urban resilience to drought, demonstrating that shaded and vegetated areas significantly enhance moisture retention compared to exposed, paved environments. Soil texture and initial moisture conditions were identified as key determinants of drought response, with finer-textured soils and wetter initial states offering greater resilience.

The study emphasizes the necessity of integrating soil moisture considerations into urban planning and climate change adaptation strategies. Enhancing green infrastructure, optimizing soil management practices, and incorporating soil moisture monitoring into urban water management can help mitigate the impacts of future drought events. Future research should focus on expanding the dataset across multiple urban locations and improving model accuracy by integrating groundwater dynamics and lateral water flow processes.

Contents

Acknowledgement v

Summary v

1 Introduction 1
1.1 Structure . . . 4

2 Methodology 7
2.1 Soil Moisture Data . . . 7
2.1.1 Measurement locations . . . 7
2.1.2 Study area . . . 7
2.1.3 Data collection . . . 8
2.1.4 Data analysis . . . 9
2.2 Soil Texture . . . 11
2.2.1 Soil sample collection . . . 11
2.2.2 Soil sample analysis . . . 12
2.3 HYDRUS-1D . . . 13
2.3.1 Settings and Boundary conditions . . . 13
2.3.2 Time variable parameters . . . 14
2.3.3 Soil profile. . . . 15
2.3.4 Optimization . . . 15
2.3.5 Drought scenario . . . 16
2.3.6 Data analysis . . . 16

3 Results 19
3.1 Soil Moisture Data . . . 19
3.1.1 Soil moisture dynamics. . . . 19
3.1.2 Interrelations between the measurement points . . . 21
3.2 Soil Texture . . . 24
3.3 HYDRUS-1D . . . 25
3.3.1 Model performance. . . . 25
3.4 Drought of 2018 . . . 30
3.4.1 Soil moisture dynamics. . . . 30
3.4.2 Effects of initial soil moisture conditions . . . 33

4 Discussion 37
4.1 Urban drought . . . 37
4.2 Urban environmental conditions . . . 37
4.3 Soil-water balance . . . 38
4.4 Limitations . . . 39

5 Conclusion 41

6 Recommendations 43

A Measurement procedure 49

B Measurement results 51

List of Figures

1.1 The four distinct types of drought defined by literature; meteorological drought, agricultural drought, hydrological drought and socioeconomic drought. Urban drought is closely related to the socioeconomic drought. The figure is adapted from Dabrowska et al. (2023). 2
1.2 The three components of evaporation are soil evaporation, transpiration and interception loss. The pie chart indicates the contribution of each process to the total evaporation process (adapted from Miralles, Brutsaert, Dolman, and Gash (2022). 3

2.1 The location of the study area at the campus of Delft University of Technology. The soil moisture content is collected at the Echo building and the weather data is obtained from The Green Village. 8
2.2 The measurement locations at the square in front of the Echo building. The description of the numbered measurement points is in Table 2.1. 8
2.3 The installation process of the access tube for the Profile Probe PR1 to measure the soil moisture content. 10
2.4 An overview of the soil sample collection next to a measurement point. The attributes needed to collect the samples are a soil drill, a shovel, a garden shovel, a measuring tape and a tool to remove the soil from the drill. 12
2.5 The wet and unprocessed soil samples compared to the dried and sieved samples. . . 12
2.6 The settings for soil profile in HYDRUS-1D. Each column has a total length of 200cm. . 15

3.1 Soil moisture dynamics of all measurement points categorized by measurement depth . 21
3.2 The correlation between the measurement points per depth, visualised in a heatmap. The bottom left triangle is for Kendall's correlation τ_b and the upper right triangle is for Spearman's correlation r_s. A darker blue color indicates a strong correlation, which fades to light blue, moderate to weak correlation. A white or red colour indicates a poor correlation between the measurement points. 23
3.3 The canopy of the trees at MP09 and MP10 straight above the measurement points. . 24
3.4 Model performance of MP01 relative to measured soil moisture content. The heatmap (a) shows Kendall's and Spearman's correlation and the bottom figure (b) illustrates soil moisture dynamics. 27
3.5 Model performance of MP02 relative to measured soil moisture content. The heatmap (a) shows Kendall's and Spearman's correlation and the bottom figure (b) illustrates soil moisture dynamics. 27
3.6 Model performance of MP03 relative to measured soil moisture content. The heatmap (a) shows Kendall's and Spearman's correlation and the bottom figure (b) illustrates soil moisture dynamics. 28
3.7 Model performance of MP05 relative to measured soil moisture content. The heatmap (a) shows Kendall's and Spearman's correlation and the bottom figure (b) illustrates soil moisture dynamics. 29
3.8 Model performance of MP08 relative to measured soil moisture content. The heatmap (a) shows Kendall's and Spearman's correlation and the bottom figure (b) illustrates soil moisture dynamics. 30
3.9 The soil moisture dynamcis for five depths at measurement points MP01, MP02, MP03, MP05 and MP08, where the drought of 2018 is considered. 33
3.10 The effect of extremely dry and wet initial soil moisture conditions on the drought pattern for MP01, MP02, MP03, MP05 and MP08. 35

B.1 Soil moisture dynamics of all measurement points categorized by measurement point. . 53

List of Tables

2.1 The measurement points number (MP##) and the corresponding description 9
2.2 Strength of the relationship for Kendall's correlation (τ_b) and Spearman's correlation (r_s) (Xiao, Ye, Esteves, & Rong, 2016). 11
2.3 The sieve numbers and corresponding mesh sizes in mm to determine the soil texture . 13
2.4 The Feddes parameters in HYDRUS-1D 14
2.5 Precipitation condition for the drought period in 2018 from April to September. 16

3.1 The soil textures for all measurement points 25

A.1 The measurement points and belonging soil type setting on the HH2 Moisture Meter . . 49

1 Introduction

Climate change is an increasing problem. Sea level rise is one of the responses to global warming that we have to deal with, along with an increased risk of floods and droughts due to more intense rainfall events and higher temperatures (Calvin et al., 2023; Ven et al., 2011). The Paris Agreement of 2016 aims to mitigate the effects of climate change globally. 175 countries agreed ”to limit the temperature increase to 1.5°C above pre-industrial levels”, by signing The Paris Agreement (UNFCC, 2016; United Nations, 2016).

The Royal Netherlands Meteorological Institute (KNMI 2023) has adapted global climate models from the IPCC 2023 to forecast regional impacts. The Netherlands will face rising temperatures, drier summers, and wetter winters (Bessembinder et al., 2023). In response, the Dutch government has primarily focused on flood prevention and water drainage, while measures addressing drought remain less developed (Bartholomeus et al., 2023; Rijkswaterstaat, 2019, 2022). Current national policies, such as the *'Landelijke maatlat'* for climate-adaptive construction, emphasize flood management strategies more comprehensively than those for drought mitigation (Rijksoverheid, 2023). This disparity highlights the need for a more balanced and proactive approach to urban drought management.

Drought is an increasingly urgent issue that affects both rural and urban areas. Given that the majority of the global population resides in cities (Aboagye & Sharifi, 2024; X. Zhang et al., 2019), and approximately 74% of people in The Netherlands live in urban environments (Nabielek & Hamers, 2015), the consequences of urban drought will be experienced by most people. Unlike floods, which produce immediate and visible damage, urban drought develops gradually and can be equally or even more disruptive (Bartholomeus et al., 2023; Dabrowska et al., 2023). It directly affects various aspects of city life, including industrial productivity, agricultural output, and public health (Dabrowska et al., 2023; X. Zhang et al., 2019). While urban drought has historically received less attention than floods, it has gained increasing recognition in the literature over the past decade (Nalau & Verrall, 2021; X. Zhang et al., 2019).

The consequences of drought in urban areas are varied and adverse, affecting both the environment and infrastructure. Urban drought leads to a decrease in groundwater levels, which can be particularly damaging to historic buildings with wooden foundation piles since they deteriorate when exposed to oxygen frequently (Albers et al., 2015; Ven et al., 2011). Additionally, declining groundwater levels accelerate soil subsidence, a natural process occurring in certain areas of the Netherlands (Ven et al., 2011). In the literature, drought is categorized into four distinct types, with urban drought being closely linked to socioeconomic drought. Unlike other types, socioeconomic drought is defined by its monetary impact rather than physical processes, further highlighting the economic and infrastructural challenges posed by urban drought (Dabrowska et al., 2023; Keyantash, 2021).

1. **Meteorological drought**: a shortage of precipitation (Keyantash & Dracup, 2002).
2. **Agricultural drought**: a shortage of available water for plant growth (Keyantash & Dracup, 2002).
3. **Hydrological drought**: a lack of water supply volume, including streamflow, reservoir storage, and groundwater level (Keyantash & Dracup, 2002).

4. **Socioeconomic drought**: a combination of the other droughts, it is tied to a monetary value and is linked to the supply and demand of economic goods (X. Zhang et al., 2019)

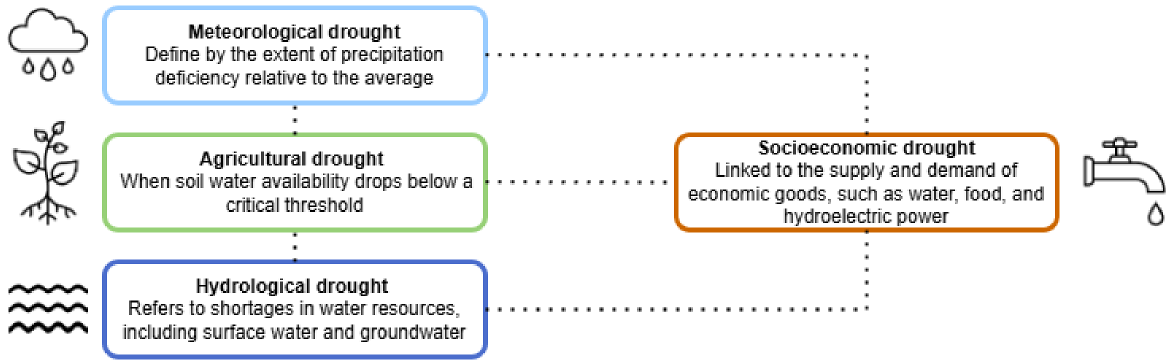

Figure 1.1: The four distinct types of drought defined by literature; meteorological drought, agricultural drought, hydrological drought and socioeconomic drought. Urban drought is closely related to the socioeconomic drought. The figure is adapted from Dabrowska et al. (2023).

Drought is a complex phenomenon, characterized by various types and their potential combinations, illustrated by Figure 1.1. Currently, the KNMI (2024) measures drought severity based on precipitation shortages, which only accounts for meteorological drought. However, this approach does not address the other types of drought. Keyantash and Dracup (2002) identify several indices that can be used to assess meteorological, agricultural, and hydrological droughts. Among these, soil moisture content is particularly effective in capturing all three types (Berg & Sheffield, 2018). Drought related to soil moisture content can be understood as the result of a time-integrated balance between precipitation deficits and subsequent surface water losses, including plant transpiration, soil evaporation, drainage to the subsurface, and runoff to lakes and rivers (Berg & Sheffield, 2018).

Urban green spaces play a critical role in climate adaptation by enhancing water infiltration during heavy rainfall, reducing strain on sewer systems (Frank Lee, 2021). Additionally, they help to mitigate the urban heat island effect by absorbing heat, offering shade and raising humidity that maintains surrounding surface and air temperatures (Jenerette, Harlan, Stefanov, & Martin, 2011; Paudel & States, 2023). These cooling effects also contribute to lower building energy consumption, leading to economic benefits and reduced greenhouse gas emissions (Paudel & States, 2023; B. Zhang, Xie, Gao, & Yang, 2014). Beyond environmental advantages, urban green spaces offer social and health benefits, improving the overall well-being (Bush & Doyon, 2019; Kabisch, Frantzeskaki, & Hansen, 2022; Kumar et al., 2021; Y. Zhang, Van den Berg, Van Dijk, & Weitkamp, 2017).

To optimize the effectiveness of green spaces, understanding soil-water dynamics is essential. The soil-water balance equation provides valuable insights into the movement of water within a defined soil volume (Z. Li et al., 2019) and is expressed as follows

$$\left[\frac{\partial S}{\partial t}\right]_0^r = P + I + W - ET - R - D \tag{1.1}$$

where P is precipitation, I is irrigation (which is limited by the hydrodynamics described in Richard's equation (Richards, 1931)), W represents the contribution from the water table upward, ET is evapotranspiration determined using the Penman-Monteith method (Daly & Porporato, 2006), R is surface runoff, D is drainage, and $\frac{\partial S}{\partial t}$ represents soil water storage in the soil layer where the roots are active to supply water to the plant (Rana & Katerji, 2000). The change in soil water storage is directly related to the soil moisture content by the following equation,

$$\left[\frac{\partial S}{\partial t}\right]_0^r = nZ_r\frac{\partial s}{\partial t} \tag{1.2}$$

where s is the vertically averaged relative soil moisture, n is soil porosity, and Z_r is the root zone depth (Daly & Porporato, 2006).

In addition to soil moisture dynamics, ET plays a crucial role in the soil-water balance and is influenced by weather conditions, the type of urban green space, and the broader urban environment. ET can be estimated using the Penman-Monteith equation (Allen, Pereira, Raes, & Smith, 1998):

$$ET_0 = \frac{0.408\Delta(R_n - G) + \gamma\frac{900}{T+273}u_2(e_s - e_a)}{\Delta + \gamma(1 + 0.34u_2)} \tag{1.3}$$

The parameters required for the Penman-Monteith equation include air humidity, air temperature, wind speed, and radiation (Allen et al., 1998). Except for air humidity, these factors are influenced by urban environmental conditions. The urban heat island effect contributes to higher temperatures (Jiang, Huang, & Sha, 2018), represented as T in $[^\circ C]$. Net solar radiation, R_n in $[MJ/m^2d]$, is crucial for determining the amount of energy available for evaporation (Brown, 2000) and is affected by shadows (Heck, Coltman, Schneider, & Helmig, 2020). Wind speed, u_2 in $[m/s]$, varies significantly at the local scale due to the positioning of buildings relative to one another (Brown, 2000; Heck et al., 2020; Wang, Yang, & Kim, 2020).

These environmental influences shape evaporation patterns in urban areas, where evaporation can occur in multiple locations. Three main types of evaporation can be distinguished: evaporation from trees, evaporation from turfgrass, and evaporation from open water bodies (Peters, Hiller, & McFadden, 2011). Evaporation, by definition, is the process in which a substance transitions from the liquid phase to the vapour phase (Miralles et al., 2022). In urban green spaces, this process consists of three key components, visualised in Figure 1.2, all contributing to the total evaporation in cities (Miralles et al., 2022) :

1. **Transpiration**: water evaporates from inside the leaves.
2. **Soil evaporation**: water evaporates from the soil .
3. **Interception loss**: evaporation of the intercepted precipitation.

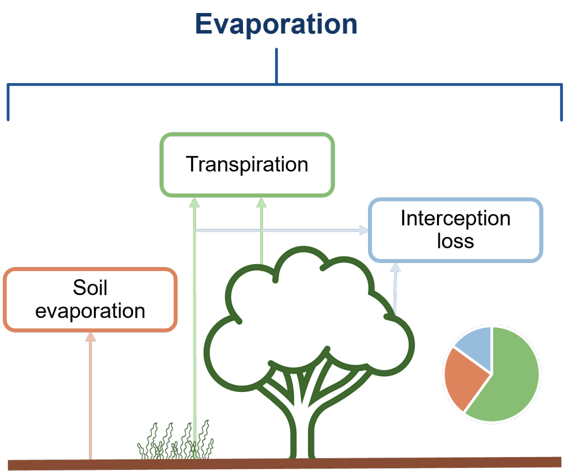

Figure 1.2: The three components of evaporation are soil evaporation, transpiration and interception loss. The pie chart indicates the contribution of each process to the total evaporation process (adapted from Miralles et al. (2022).

The most critical component of the evaporation process is the availability of water, as evaporation cannot occur without it (Brown, 2000). When sufficient soil moisture is present, three additional factors influence evaporation: plant type, stage of plant development, and weather conditions (Brown, 2000). The evaporation rate varies depending on the plant species, with native plants being more adapted to local conditions and generally requiring less water than non-native species (Brown, 2000; Peters et al., 2011). Additionally, plant growth and activity stages determine water usage, as actively growing plants consume significantly more water than dormant ones (Brown, 2000). Finally, weather conditions also play a crucial role, as previously explained in the context of the Penman-Monteith equation.

Since plants play a key role in the evaporation process, understanding root water uptake is essential. It is a complex process influenced by multiple factors, including water availability, plant water status, and root architecture (Nguyen, Joshi, & Kant, 2017). Root water uptake occurs passively, driven by a water potential gradient caused by leaf transpiration (Steudle & Peterson, 1998). The amount of water a plant can absorb depends on root hydraulic conductivity, which determines how effectively roots can extract water from the soil (Nguyen et al., 2017). To quantify this process, Feddes, Kowalik, Kolinska-Malinka, and Zaradny (1976) developed a method that estimates root water uptake as a function of soil water content, providing valuable insights into how plants access and utilize soil moisture.

The root water uptake in a 1D root system can be approached by the following equation,

$$\frac{\partial \theta}{\partial t} = -\frac{\partial v_z}{\partial z} - S_z \tag{1.4}$$

where z represents the vertical coordinate (positive upward) in $[cm]$, v_z is the Darcian soil water-flux density (positive upward) in $[cm/d]$, and S_z denotes the root water uptake rate in $[cm^3/cm^3 d]$. The uptake process is influenced by root density, soil water pressure head, depth and time, either independently or in combination (Feddes & Raats, 2004). In most cases, it is assumed that in unsaturated soil, water movement occurs predominantly in the vertical direction z (Feddes & Raats, 2004).

To predict root water uptake patterns, it is essential to consider the hydraulic conductivity, $k(h)$, along with the profiles of hydraulic head, h, and soil moisture, θ (Feddes & Raats, 2004). These properties are strongly influenced by soil texture (Nelson & Miller, 1997; Vorwerk, Cameron, & Keppel, 2015). A study by N. Li, Skaggs, Ellegaard, Bernal, and Scudiero (2024) highlights the significant impact of soil texture on soil moisture dynamics. As depth increases, soil texture plays an increasingly crucial role in moisture distribution. Textures such as clay-loam, silt-clay, and silt-loam exhibit better moisture conductivity between surface and deeper soil layers, improving water availability for plant roots (N. Li et al., 2024). In contrast, sandy soils, with larger pores and lower water-holding capacity, drain surface water quickly, leading to low soil moisture retention. On the other hand, clayey soils retain more water in both surface and deeper layers, ensuring greater soil moisture availability over time (N. Li et al., 2024).

Urban green spaces are widely used to mitigate the effects of climate change, particularly by reducing flooding and the urban heat island effect. However, the impact of urban green spaces concerning drought is little knowledge about (Bartholomeus et al., 2023; Yimer et al., 2024). Drought, especially in urban areas, is a complex phenomenon influenced by multiple factors, such as weather, urban environments, and vegetation types. One key indicator of drought is soil moisture content, which can reflect meteorological, agricultural, and hydrological drought conditions. A combination of these droughts forms together the socioeconomic drought, which is closely linked to urban drought. Despite the growing importance of this issue, there is still much to learn about the interactions between soil moisture, vegetation, and urban environments in shaping drought conditions. Therefore, the aim of this research is:

To identify the relationship between green spaces in urban areas and soil moisture dynamics in relation to drought.

This is achieved by answering the following research questions:

- How do urban environmental conditions affect soil moisture content in green spaces?
- What is the effect of soil texture on soil moisture dynamics?
- How do initial soil moisture conditions influence soil moisture dynamics during a drought period, as modelled using HYDRUS-1D?

1.1. Structure

The following Chapter 2 discusses the methodology for this research, firstly, the collection of soil moisture data at the study site is explained. This is followed by the soil texture determination. The final section of this chapter introduces the HYDRUS-1D model used to model the soil moisture dynamics, which is used to simulate drought for different initial soil moisture conditions. The results of this research are explained in Chapter 3. The meaning of the results in a broader context is discussed in Chapter 4, together with the limitations of this research. Finally, Chapter 5 summarizes the findings of this research, ending with recommendations for future research in Chapter 6

2
Methodology

This chapter describes the methods used to answer the research questions, focusing on soil moisture data collection, soil texture determination, and modeling soil moisture dynamics in HYDRUS-1D. First, the soil moisture data collection process is explained, including details on the study area and sensor usage at five locations on the campus of Delft University of Technology. Next, the method for determining soil texture at each of these locations is described. Finally, the HYDRUS-1D model is introduced, where extreme initial soil moisture conditions are applied to simulate a drought scenario and analyze soil moisture dynamics under varying conditions.

2.1. Soil Moisture Data

The soil moisture data is collected at the campus of Delft University of Technology at the square in front of the Echo building. This area has all urban environmental conditions within a radius of 200m. The data is collected manually, 3 to 4 times per week during the measurement period, starting from July 20th till September 30th 2024, with a total amount of 33 measurements.

This section explains the study area in more detail, followed by the measurement locations. Thirdly, the data collection and the belonging sensor are explained. The final part of this section explains the analysis of the collected soil moisture contents.

2.1.1. Measurement locations

The urban environmental conditions are determined based on the soil-water balance equation, the evaporation process and the root water uptake, as explained in Chapter 1. Five urban environmental conditions are selected, areas with sun, shadow, grass, trees and pavement. For each of the urban environmental conditions, a control group is placed in the study area as well, so a total of 10 measurement locations are allocated. The function of the control group is to verify the data from the corresponding measurement points. In addition, the control group can be used as a fallback for the values as the measurement locations are placed in public places. Disruptions or destructions of the access tubes by people, lawnmowers or dogs are likely to occur, affecting the measurement possibilities or the accuracy. The study area is depicted in Figure 2.1, which is explained in detail in Section 2.1.2.

2.1.2. Study area

The 10 measurement points are located in front of the Echo building, the area was recently (re)developed and completed in 2022. The exact locations of the measurement points are shown in Figure 2.2 and the belonging abbreviations are in Table 2.1. As part of this redevelopment, the groundwater level for the site was established at -3.02 m below NAP (Hoogheemraadschap Delfand, 2024), while the ground level ranges between -0.5 m and -1.02 m below NAP (AHN, 2024). During the redevelopment, a new sewer system was constructed, with the guidelines outlined in *Technische Programma van Eisen voor de inrichting van de openbare ruimte van de TU Delft; Module 6: Riolering* (Corovum Advies B.V., 2018). This area features a separate sewer system comprising the following components: sanitary

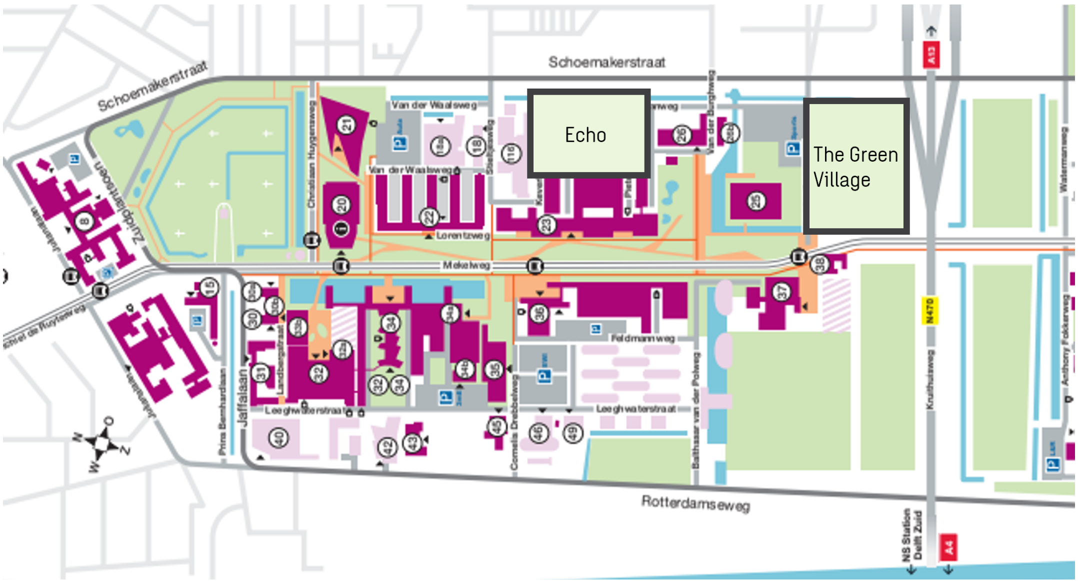

Figure 2.1: The location of the study area at the campus of Delft University of Technology. The soil moisture content is collected at the Echo building and the weather data is obtained from The Green Village.

sewer system, stormwater sewer system, and fire sewer system. The sanitary sewer system collects wastewater from households and businesses and directs it to a treatment plant. The stormwater sewer system is divided into two parts: a stormwater system that prevents flooding by discharging excess rainwater, and a drainage and infiltration sewer system that facilitates water infiltration, contributing to groundwater recharge. The fire sewer system is exclusively used in case of a fire emergency.

Figure 2.2: The measurement locations at the square in front of the Echo building. The description of the numbered measurement points is in Table 2.1.

2.1.3. Data collection

The soil moisture content at each measurement point is measured using a Profile Probe PR1 in combination with the HH2 Soil Moisture Meter, both manufactured by Delta-T Devices. The Profile Probe PR1 can measure the soil moisture content at six depths: 100mm, 200mm, 300mm, 400mm, 600mm, and 1000mm. The HH2 Moisture Meter supplies power to the Profile Probe PR1 and measures the

Table 2.1: The measurement points number (MP##) and the corresponding description

MP	Description
MP01	Grass shadow
MP02	Grass sun
MP03	Grass sun
MP04	Grass shadow
MP05	Grass shadow
MP06	Paved
MP07	Paved
MP08	Grass sun
MP09	Tree
MP10	Tree

output signal in Volts (Bavel van & Nichols, 2002). These Volts are converted to soil moisture values in %, depending on the set soil type.

During the measurements, the values were collected using the generic settings for either organic or mineral soil types. This is because the soil texture for each measurement point was only determined after the measurement period. The soil moisture content is calculated using the following equation

$$\sqrt{\varepsilon} = a_0 + a_1\theta \tag{2.1}$$

where ε is the dielectric constant, a_0 and a_1 are soil parameters and θ represents the measured soil moisture (Bavel van & Nichols, 2002; Delta-T Devices Ltd., 2017). The generic settings allow for a soil moisture content measurement range from 0% to 100%.

The Profile Probe PR1 operates by being inserted into access tubes that are permanently installed in the soil. These access tubes allow for repeated measurements at the same location throughout the measurement period. The installation process, depicted in Figure 2.3, involves manually drilling a hole to the required depth and diameter. To ensure a tight fit between the access tube and the surrounding soil, which is crucial for accurate measurements, a water-soil mixture is used as a lubricant during the installation.

Once installed, the access tubes remain in place for the entire measurement period. Each measurement consists of three readings for all depths, with the Profile Probe PR1 rotated by 120° between each reading. This rotational approach ensures a comprehensive assessment of soil moisture conditions across all depths. The detailed measurement procedure is outlined in Appendix A

2.1.4. Data analysis

The analysis of the collected soil moisture content comprises multiple stages. Initially, the data is prepared by calculating the average soil moisture value for each measurement point. Following this preparation, the data undergoes both visual and statistical analysis.

The visual analysis is conducted using two distinct approaches. The first approach examines soil moisture dynamics at individual measurement points, offering localized insights. The second approach analyzes soil moisture dynamics across different depths for all measurement points, providing a broader perspective on moisture distribution patterns.

The statistical analysis is used to quantify the relationship between the measurement points, Spearman's correlation and Kendall's correlation are applied. These tests assess the presence of a monotonic trend between datasets based on ranks, making them suitable alternatives to Pearson's correlation, which requires normally distributed data (Learn Statistics Easily, 2024; Puth, Neuhäuser, & Ruxton, 2015; Xiao et al., 2016). While both Spearman's and Kendall's tests are appropriate, Kendall's correlation is preferred in the analysis due to its greater robustness against outliers (Learn Statistics Easily, 2024; Puth et al., 2015). This ensures a more reliable assessment of the interrelations between measurement points.

(a) The installation of the access tube

(b) The access tube fully installed into the soil

Figure 2.3: The installation process of the access tube for the Profile Probe PR1 to measure the soil moisture content.

Kendall's correlation

Kendall's correlation τ compares two measurement units, evaluating whether the ranks of pairs move in the same direction. Given two pairs of observations (x_i, y_i) and (x_j, y_j) are said to be concordant if the ranks for both elements agree to increase or decrease: ($x_i > x_j$ and $y_i > y_j$) or ($x_i < x_j$ and $y_i < y_j$). They are discordant if one value increases while the other decreases: ($x_i > x_j$ and $y_i < y_j$) or ($x_i < x_j$ and $y_i > y_j$). If ($x_i = x_j$ and/or $y_i = y_j$), the pair is neither concordant nor disconcordant (Puth et al., 2015; Xiao et al., 2016). Kendall's rank correlation, for a sample size n, is calculated for the most commonly used τ_b

$$\tau_b = \frac{n_c - n_d}{\sqrt{(n_0 - n_1)(n_0 - n_2)}} \tag{2.2}$$

where n_0 are unique unorded pairs of observations (n_0 = 0.5$n(n-1)$). Let n_c be the number of concordant pairs and n_d the number of discordant pairs. The tied values in X and Y are represented by n_1 and n_2,

$$n_1 = 0.5 \sum_{i=1}^{q} t_i(t_i - 1), \quad n_2 = 0.5 \sum_{j=1}^{q} u_i(u_i - 1) \tag{2.3}$$

where t_i and u_j represent the number of tied values for each group for X and Y, respectively.

The resulting τ_b values fall within a range -1 ≤ τ_b ≤ 1. A higher absolute value indicates a stronger association. Where a positive τ_b suggests that higher values of one variable are associated with higher values of the other and a negative τ_b suggests that higher values of one variable correspond to lower values of the other (Puth et al., 2015). A correlation of $\tau_b \geq 0.4$ is considered as being strong during the analysis (Xiao et al., 2016). An overview of the deviation of strength for the values is in Table 2.2.

Spearman's correlation
Spearman's correlation is conceptually similar to Person's correlation but applied to ranked data rather than raw values. It measures the strength and direction of a monotonic relationship between two ranked variables (Puth et al., 2015; Xiao et al., 2016). The Spearman's correlation coefficient, r_s, can be calculated with

$$r_s = 1 - \frac{6 \sum d_i^2}{N(N^2 - 1)} \tag{2.4}$$

where $d_i = X_i' - Y_i'$ is the difference between the ranks of corresponding observations in the two datasets and N is the total number of samples. In the analysis, only positive values of $r_s \geq 0.4$ are considered as a strong relationship, between measurement points, similar to Kendall's correlation (Puth et al., 2015; Xiao et al., 2016).

Table 2.2: Strength of the relationship for Kendall's correlation (τ_b) and Spearman's correlation (r_s) (Xiao et al., 2016).

Correlation Value ($\|r\|$)	**Relationship Strength**
0.80 – 1.00	Very strong
0.60 – 0.79	Strong
0.40 – 0.59	Moderate
0.20 – 0.39	Weak
0.00 – 0.19	Very weak

2.2. Soil Texture

Soil texture is categorized into three main types: clay, sand, and silt. Each texture or combination of textures affects the ease with which soil can be worked, the amount of water and air it holds, and the rate at which water can enter and move through soil (FAO, 2006; Rabot, Wiesmeier, Schlüter, & Vogel, 2018). The behaviour of the soil texture is primarily governed by the soil water retention curve (Rabot et al., 2018). To achieve a comprehensive understanding of soil moisture dynamics, the soil texture at each measurement point is determined. Additionally, this information is essential for input into the HYDRUS-1D model.

2.2.1. Soil sample collection

The soil texture is assessed at four depths: 15cm, 30cm, 50cm and 80cm across all measurement locations. These depths are selected based on multiple aspects. First of all, the top layer is expected to contain a high amount of organic material, while the remaining depths correspond to the Profile Probe measurement depths and the limitations of the available drill. Figure 2.4 illustrates the materials used for collecting soil samples at these depths.

Figure 2.4: An overview of the soil sample collection next to a measurement point. The attributes needed to collect the samples are a soil drill, a shovel, a garden shovel, a measuring tape and a tool to remove the soil from the drill.

2.2.2. Soil sample analysis

The collected soil samples are stored and labelled in plastic bags before the start of the drying process. The soil texture is determined by the laboratory test for textural classes (FAO, 2006). To ensure all moisture is evaporated while avoiding the burning of organic material, the samples are oven-dried for 24 hours at a temperature of 105°C. After drying, the soil is sieved through six sieves of varying mesh sizes, as listed in Table 2.3. Particles that cannot pass through the largest mesh are excluded from further analysis. The remaining soil is sieved through all mesh sizes, and the texture is determined by measuring the weight of soil retained in each sieve relative to the total sample weight.

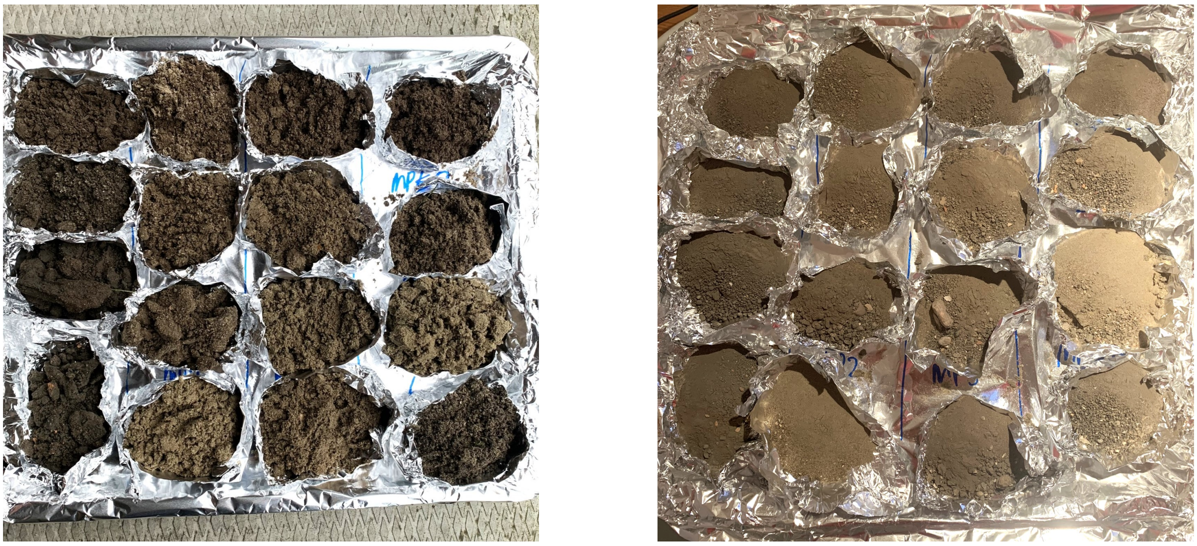

(a) Wet and unprocessed samples.

(b) Dried and sieved samples.

Figure 2.5: The wet and unprocessed soil samples compared to the dried and sieved samples.

Table 2.3: The sieve numbers and corresponding mesh sizes in mm to determine the soil texture

Sieve #	Mesh size [mm]
1	1.940
2	0.930
3	0.466
4	0.263
5	0.122
6	0.055

2.3. HYDRUS-1D

HYDRUS-1D is used to simulate the soil moisture dynamics under the same conditions as the measurement locations. While HYDRUS-2D/3D are commercially available, this research focuses solely on HYDRUS-1D due to its free accessibility (PC -Progress, 2021). The model is used to apply a drought scenario to the measurement points while having different initial soil moisture conditions.

The governing water flow equation in HYDRUS-1D is the modified Richards equation:

$$\frac{\partial \theta}{\partial t} = \frac{\partial}{\partial x}\left[K(h)\frac{\partial h}{\partial x}\right] + \frac{\partial K(h)}{\partial x} - S(h) \tag{2.5}$$

where h is the water pressure head $[L]$, θ is the volumetric water content $[L^3L^{-3}]$, t is time $[T]$, x is the vertical coordinate axis $[L]$ (positive in the opposite direction to gravity), $S(h)$ is a water sink term $[L^3L{-}3T^{-1}]$ and $K(h)$ is the hydraulic conductivity (Valentine & Apelt, 2011).

This section first outlines the settings and boundary conditions of the model, followed by a description of the model optimization process. Subsequently, the characteristics of drought and extreme initial soil moisture conditions are examined. Finally, the model results are evaluated against the measurements, with a focus on assessing the impact of extremely dry and wet initial soil moisture conditions on drought development.

2.3.1. Settings and Boundary conditions

The van Genuchten-Mualem equation describes the relationship between hydraulic conductivity $K(h)$ and soil water content where,

$$\theta(h) = \begin{cases} \theta_r + \frac{\theta_s - \theta_r}{[1+|\alpha h|^n]^m} & h < 0 \\ \theta_s & h \geq 0 \end{cases} \tag{2.6}$$

$$K(h) = K_s S_e^l \left[1 - \left(1 - S_e^{\frac{1}{m}}\right)^m\right]^2 \tag{2.7}$$

where the effective saturation, S_{es}, is

$$S_e = \frac{\theta - \theta_r}{\theta_s - \theta_r} \tag{2.8}$$

$$m = 1 - \frac{1}{n}, \quad n > 1 \tag{2.9}$$

here, θ_r and θ_s are the residual and saturated water content, K_s represents the saturated hydraulic conductivity, while α, n and l are empirical parameters governing the shape of the soil water retention curve. Specifically, α is related to the inverse of the air entry suction, where n and l describe the pore size distribution and pore connectivity (Caiqiong & Jun, 2016; Chen, Willgoose, & Saco, 2014; Valentine & Apelt, 2011). Within the van Genuchten-Mualem equation, hysteresis in the retention curve and conductivity with an initially drying curve are assumed.

Soil hydraulic parameters
The soil hydraulic parameters are derived from soil texture using the Rosetta neural network prediction function within HYDRUS-1D (Šimůnek, Van Genuchten, & Šejna, 2012). The identified soil textures serve as input values for determining these parameters. The methodology for determining soil texture at each measurement point is detailed in Section 2.2.

Boundary conditions
The upper water flow boundary condition depends on land cover, for vegetated areas, Atmospheric BC with Surface Layer is assumed and for paved areas, Atmospheric BC with Surface Runoff. In the lower boundary condition, Horizontal Drains are used to simulate lateral outflow at most measurement points. This approach assumes a homogeneous soil profile with a drainage layer positioned above an impervious layer. The initial conditions for the model are specified in terms of water content, using the first measured soil moisture values.

Root water uptake
The root water uptake is based on the Feddes approach,

$$S(h) = \beta(h)S_p \tag{2.10}$$

where $\beta(h)$ is the root-water uptake stress response function, and S_p represents the potential root water uptake rate $[T^-1]$ (Chen et al., 2014; Šimůnek et al., 2012). The ability of roots to absorb water varies with the soil's pressure head (h) (Feddes & Raats, 2004). When the soil is almost saturated, the anaerobiosis point P_0, the root water uptake is close to zero. The root water uptake is reaching its maximum efficiency between the optimal pressure head $(P_{opt)})$ and P_2, where vegetation can access water freely. Between $P2$ and $P3$, the root water uptake rate gradually declines as water availability diminishes. Eventually, when the pressure head drops below P_3, the soil reaches the wilting point, where plants no longer extract water, leading to severe water stress. Table 2.4 explains all the parameters that are required by HYDRUS to calculate the root water uptake, using Feddes. The values for these parameters are from the database provided by the HYDRUS-1D and Šimůnek et al. (2012).

Table 2.4: The Feddes parameters in HYDRUS-1D

Feddes Parameter	Description
P0	Pressure head below which roots begin water extraction
POpt	Pressure head below which water extraction is at the maximum rate
P2H	Limiting pressure head at maximum water uptake (high transpiration rate)
P2L	Limiting pressure head at maximum water uptake (low transpiration rate)
P3	Wilting point pressure head, which is below water uptake ceases
r2H	Potential transpiration rate $[LT^{-1}]$
r2L	Potential transpiration rate $[LT^{-1}]$

2.3.2. Time variable parameters

The time variable parameters in HYDRUS-1D are meteorological parameters. The specific parameters required for the simulation depend on the model settings. For this model, the input parameters are precipitation $[cm/day]$, potential evaporation $[cm/day]$, hCrtitA $[cm]$, and potential transpiration $[cm/day]$.

The potential evapotranspiration, ET_P is calculated with Penman-Monteith. The potential evapotranspiration is split into potential soil evaporation, E_p, and interception evaporation, T_p, using Beer's Law (Chen et al., 2014; Valentine & Apelt, 2011),

$$E_p = ET_p \cdot exp(-rExtinct \cdot LAI) \tag{2.11}$$

$$T_P = ET_P - E_P \tag{2.12}$$

where $rExtinct$ represents the radiation extinction coefficient and LAI is the Leaf Area Index. This partitioning helps model how much moisture is lost directly from the soil versus how much is taken up by plants through transpiration.

2.3.3. Soil profile

In HYDRUS-1D, the soil profile is defined by material layers, root distribution, and initial water content. In this study, the soil profile is constructed using four distinct material layers, as identified in Section 2.2. Figure 2.6 provides an overview of the soil settings for a measurement point, where each column has a length of 200 cm.

Root distribution varies depending on vegetation type at each measurement point. For grass-covered areas, roots are assumed to extend only within the top 20cm of soil, with a non-linear distribution concentrated near the surface. The initial soil moisture conditions are based on the first recorded measurements. Between the measurement depths, a linear interpolation of soil moisture content is applied to estimate the initial distribution.

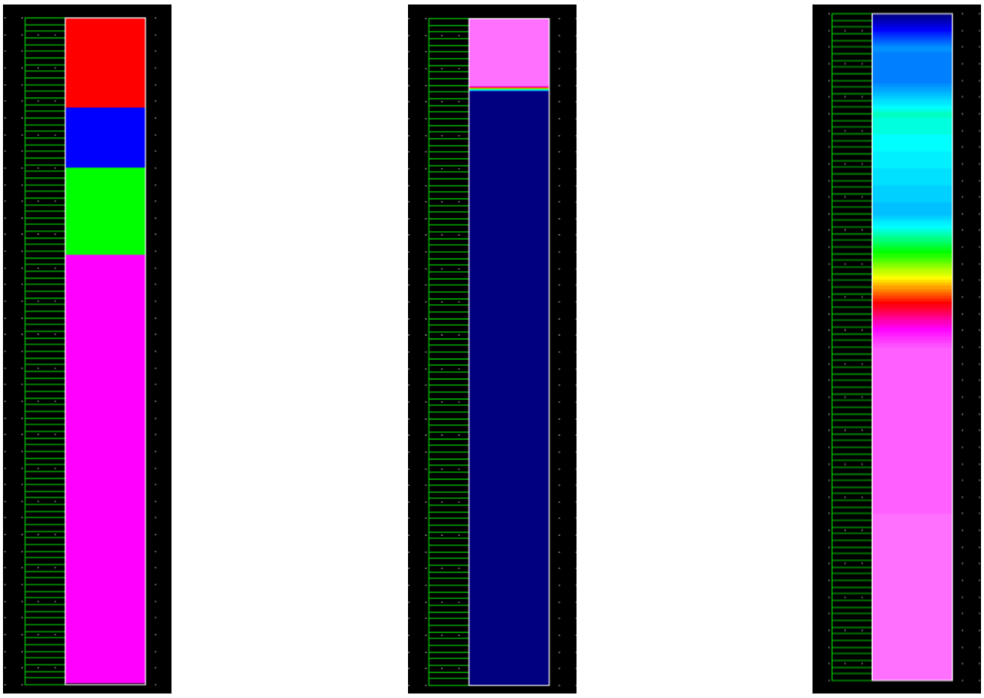

(a) A soil column in HYDRUS-1D, where each colour represents a different soil material.

(b) The root distribution of the grass. The pink color represents the roots of the vegetation and the blue color means no roots

(c) The water content distribution over the soil column based on the first measurement. No soil moisture is assumed at the top layer and the soil is fully saturated at the bottom.

Figure 2.6: The settings for soil profile in HYDRUS-1D. Each column has a total length of 200cm.

2.3.4. Optimization

The optimization of the model performance is performed by Monte Carlo simulations using a uniform distribution for the possible soil hydraulic parameters. The model's performance is primarily influenced by the Van Genuchten-Mualem parameters α, n and the hydraulic conductivity K (Ouédraogo, Berthier, Sage, & Gromaire, 2025).

The values of the Monte Carlo simulations are constrained by the range of the soil hydraulic parameters. A total of 10.000 simulations are performed to identify the optimal combination of these parameters. The best configuration is selected based on Spearman's rank correlation with the corresponding measurement point. A more detailed explanation of the selection process can be found in Section 2.3.6.

2.3.5. Drought scenario

The HYDRUS-1D model is used to model drought with extreme initial soil moisture conditions. In the Netherlands, the dry period typically spans from April to September (Bessembinder et al., 2023). The year 2018 is recognized as one of the driest in recent years, and detailed information about the drought, dry spells, and precipitation during that dry period is provided in Table 2.5. Meteorological data from 2018 is used to calculate the necessary variables, as described in Section 2.3.2. Droughts like the one in 2018 are expected to become more frequent in the future due to climate change (KNMI, 2023).

To determine the impacts of the urban environmental conditions on drought development, the model begins with the initial measured soil moisture contents. This is followed by applying both extremely dry and wet initial soil moisture conditions. These extreme values are determined manually to ensure the model converges properly.

Table 2.5: Precipitation condition for the drought period in 2018 from April to September.

Metric	**Value**
Dry spell period	54 days
Total precipitation	359.4 mm
Average precipitation	1.96 mm/day

2.3.6. Data analysis

The data analysis of the model aims to assess its performance and investigate the influence of urban environmental conditions and initial soil moisture content on drought development. Accordingly, the analysis is divided into two main components: an assessment of model performance and an investigation into the influence of urban environmental conditions on the 2018 drought, as well as the impact of extremely dry and wet initial soil moisture conditions on soil moisture dynamics during this period.

Model performance

The model performance aims to identify the best model for each corresponding measurement point. This selection process relies on the same statistical analyses, Kendall's and Spearman's correlation, as used in the Section 2.1.4 to assess the interrelation between the measurement points. These correlation methods are appropriate here too, because the scales for verifying the model against measurements differ. The measurements range from 0% to 100%, reflecting the settings of the sensor, while the calculated values from HYDRUS-1D are bounded by field capacity, typically ranging from around 5% to 50%.

Similar to the analysis in Section 2.1.4, Kendall's correlation τ_b is leading over the values of Spearman's correlation r_s. A correlation value of τ_b and $r_s \geq 0.4$ is considered a strong correlation, with any deviation between the two values shown in Table 2.2. Model performance is assessed by comparing measured and modeled soil moisture dynamics using these correlation methods, which are well-suited for handling the differing measurement scales between observed and simulated soil moisture contents, explained in Section 2.3.6. Measured soil moisture is derived from sensor voltage readings and soil water retention curves specific to each soil texture (Bavel van & Nichols, 2002; Delta-T Devices Ltd., 2017). However, since the soil moisture sensors use generic calibration settings rather than texture-specific properties, absolute values may not fully reflect site-specific soil characteristics. Despite this, the strong linear component of soil water retention curves minimizes the impact of scale differences on soil moisture dynamics.

During model performance analysis, the topsoil layers at depths 100mm, 200mm and 300mm are prioritized over the deeper layers. This is because the model does not account for groundwater effects, which can be influenced by groundwater uplift. The final selection for the soil hydraulic parameters is based on the visual performance of the model compared to the measurements, based on the researcher's judgement.

Drought of 2018

The drought of 2018 is applied to the measurement points to assess how the urban environmental conditions influence drought development. The analysis focuses on comparing soil moisture dynamics between sunny and shaded measurement points. To identify differences, a visual analysis of soil moisture dynamics is performed.

Furthermore, the study investigates the effects of extreme initial soil moisture conditions, both extremely dry and wet, on soil moisture dynamics during the 2018 drought. The analysis explores how drought progresses under these two scenarios and how the impact varies between sunny and shaded measurement points.

3 Results

This chapter describes the results and interpretation of this study's results, based on the outcome of the research presented in the Methodology in Chapter 2. First, the measured soil moisture content is analysed in relation to the urban environmental conditions. Next, the soil texture in relation to the soil moisture content is discussed. The last part consists of the model performance, followed by the impact of initial soil moisture conditions on drought patterns based on the drought of 2018.

3.1. Soil Moisture Data

Soil moisture data was collected across five urban environmental conditions: sun, shadow, grass, trees, and pavement, covering ten measurement points. The soil moisture analysis has been divided into two parts. The first section examines overall soil moisture dynamics in relation to weather conditions and urban settings, while the second part explores interrelations between measurement points to assess spatial variability. Due to significant disruptions during the measurement period, MP04 is excluded from the analysis.

The data was collected over ten weeks, with only two weeks without precipitation. Despite an overall precipitation deficit of 75mm, a meteorological drought classification, this summer was not among the most extreme dry summers projected under climate change scenarios (Bessembinder et al., 2023; KNMI, 2024; Yimer et al., 2024). Therefore, the measured soil moisture content serves primarily to assess the general effects of urban environmental conditions on soil moisture dynamics.

3.1.1. Soil moisture dynamics

The soil moisture dynamics at different measured depths are visualised in Figure 3.1. These figures indicate that all green measurement points (i.e., those located in vegetated areas rather than paved surfaces) respond to the weather circumstances. As expected, soil moisture levels decrease during dry periods and increase following precipitation events, with the magnitude of change depending on the duration and intensity of these weather conditions.

The soil moisture dynamics at the green measurement points exhibit a clear response to weather variations at shallow depths, 100mm to 300mm, with the magnitude of this response decreasing as depth increases. At deeper levels, 600mm and 1000mm, soil moisture responds only to extreme weather events. Extended dry periods generally lead to a decrease in moisture content, while only substantial precipitation events produce notable increases. Regular precipitation events contribute to minor changes, but these cannot be definitively attributed to individual precipitation occurrences.

From a depth of 600mm onward, differences between green measurement points become pronounced. These variations are influenced by several factors, including urban environmental conditions, soil texture, and groundwater level. The urban environmental conditions also contribute to variations in soil moisture behaviour, particularly in how vegetation interacts with infiltration and evaporation.

Paved measurement points exhibit markedly different soil moisture dynamics compared to vegetated areas. Paved surfaces consistently maintain lower soil moisture levels, with minimal responsiveness to weather variations. This is likely due to the impermeability of pavement, which restricts direct infiltration. The primary source of moisture infiltration in these areas is the small opening around the access tubes, allowing only minimal water entry.

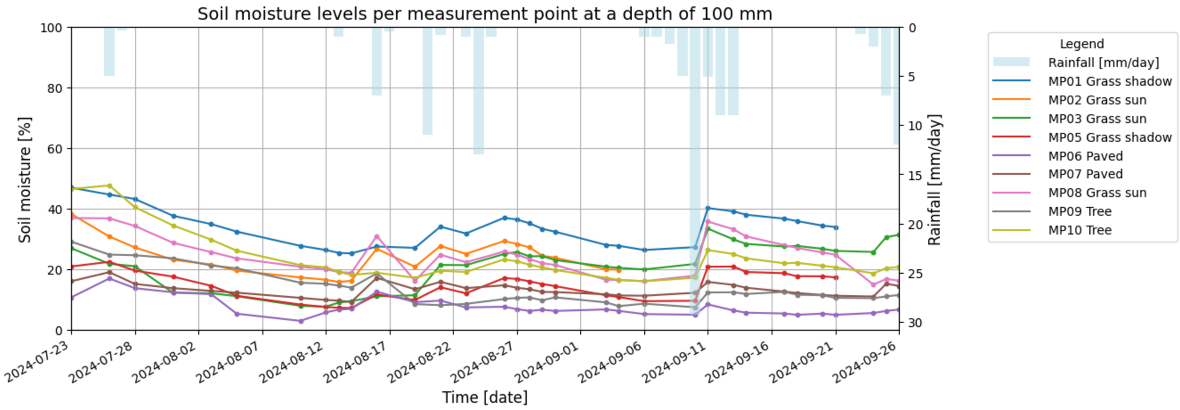

(a) Measurement depth 100mm

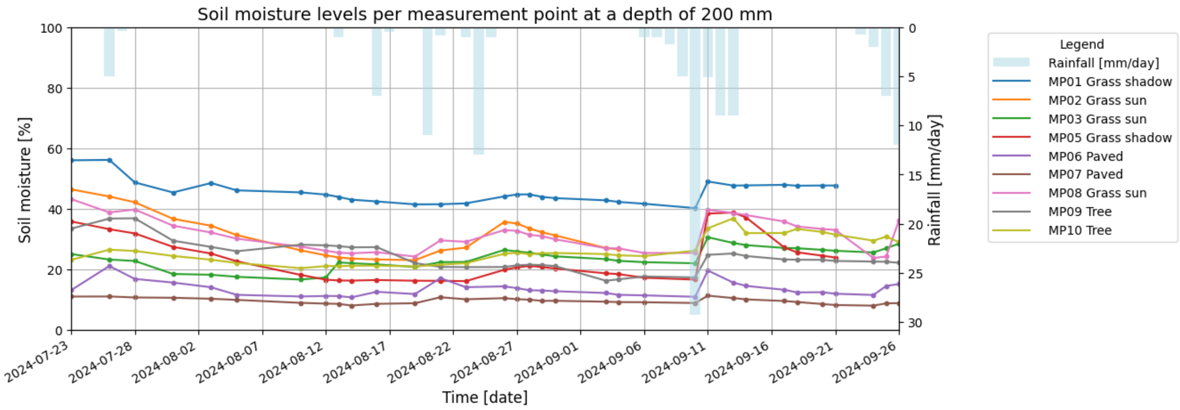

(b) Measurement depth 200mm

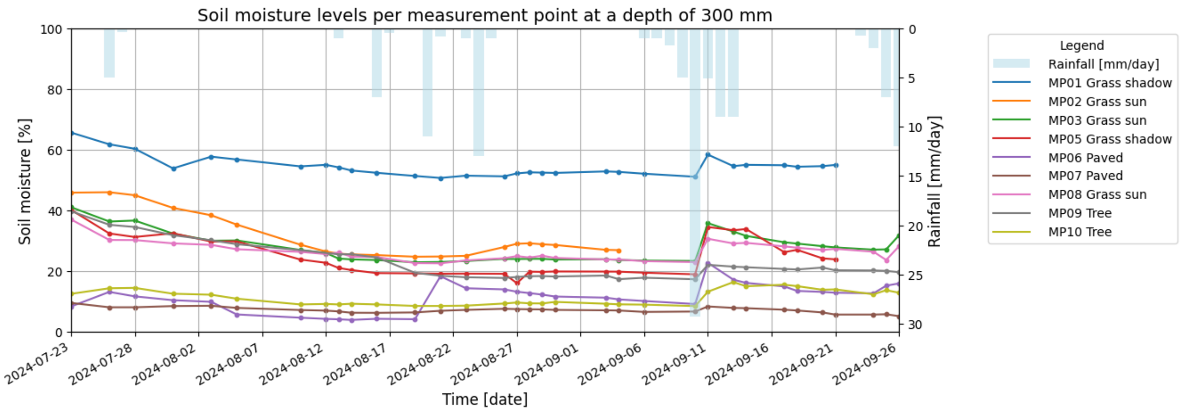

(c) Measurement depth 300mm

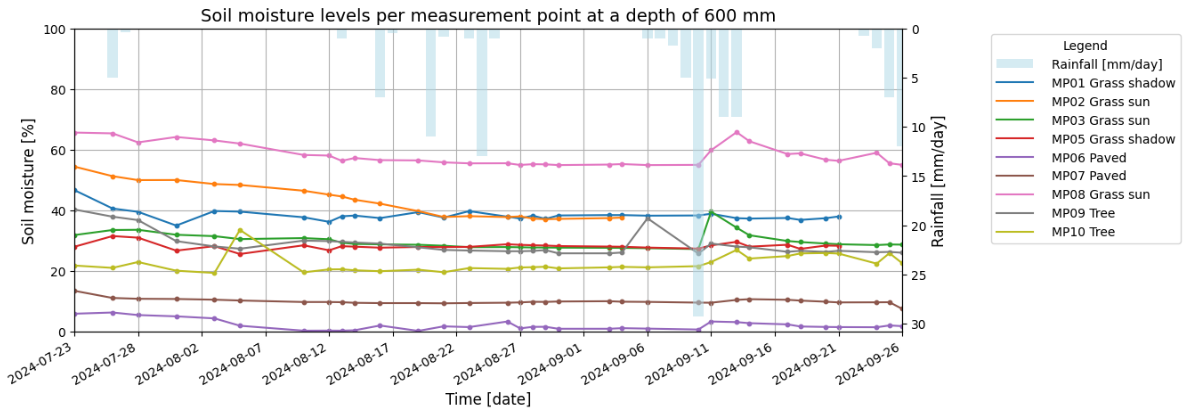

(d) Measurement depth 600mm

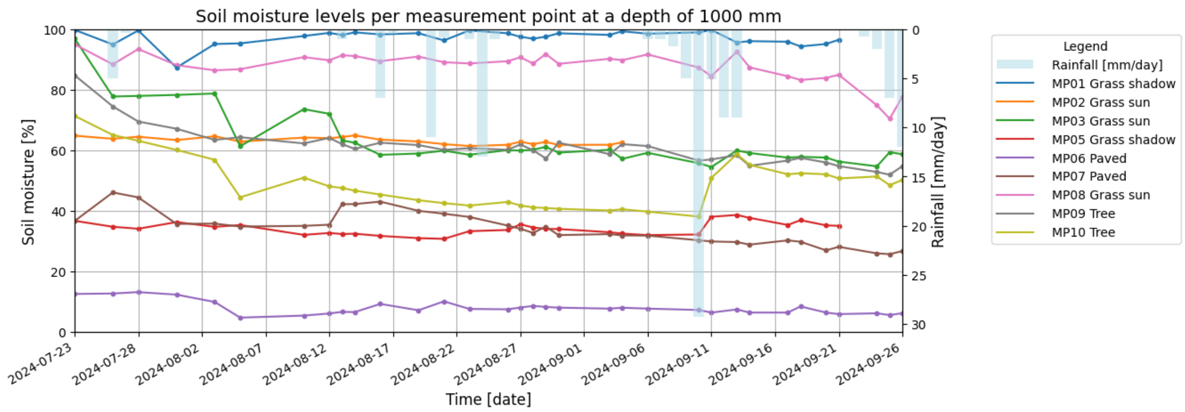

(e) Measurement depth 1000mm

Figure 3.1: Soil moisture dynamics of all measurement points categorized by measurement depth

While the manual data collection method provided valuable insights into soil moisture dynamics, it also introduced certain limitations. Measurements taken before, during, or after precipitation events could yield varying values, potentially affecting consistency. To minimize this variability, measurements were conducted at consistent times on each sampling day. Additionally, the data collection frequency—limited to three to four times per week—may have resulted in missed short-term fluctuations in soil moisture levels. Despite these limitations, the collected data provides a reliable representation of broader soil moisture dynamics and serves as a robust basis for further analysis.

The variation in soil moisture behavior across different depths underscores the influence of urban environmental conditions, soil properties, and external factors such as precipitation and groundwater levels. Additionally, the installation process of the access tubes can temporarily disrupt moisture equilibrium. As reported by Bavel van and Nichols (2002), it takes several weeks for equilibrium to be re-established, with the duration depending on soil texture, as indicated in Table 3.1. Sandy soils stabilize more quickly than clayey soils, which require a longer adjustment period. The following section further explores these patterns by analyzing correlations between measurement points to assess spatial variability and determine the extent to which different locations exhibit similar moisture dynamics.

3.1.2. Interrelations between the measurement points

The soil moisture dynamics of the five urban environmental conditions are compared across all measurement points. To assess interrelations, Kendall's correlation, τ_b, and Spearman's correlation, r_s, are applied to all possible measurement point combinations at each measurement depth. These correlations are visualized in Figure 3.2, where the bottom left triangle represents Kendall's correlation and the upper right triangle represents Spearman's correlation. A correlation value of $\tau_b/r_s \geq 0.4$ is considered as strong, as detailed in Section 2.1.4.

The analysis of interrelations between measurement points is categorised based on the urban environmental conditions: grass (sun and shaded), pavement and trees. Measurement point abbreviations and descriptions are provided in Table 2.1.

Grass
All grass-covered measurement points (MP01, MP02, MP03, MP05 and MP08), whether in sunny or shaded areas, show strong correlation depths up to 300mm. This relationship weakens at 600mm and 1000mm. Two key factors contribute to this shift in correlation strength.

First, the influence of sun and shade becomes more pronounced at the increased depths of 600mm and 1000mm. Sunny locations (MP02, MP03, MP08) continue to exhibit correlation at deeper depths, whereas shaded areas (MP01, MP05) no longer correlate with their sunny counterparts. Additionally, a weak correlation is observed within the shaded areas themselves, likely due to differences in soil texture between MP01 and MP05, see Table 3.1.

The second factor is groundwater uplift, which varies across the study area depending on soil texture. Since groundwater movement influences soil moisture at deeper depths, variations in soil textures create differences in soil moisture dynamics among measurement points, mainly visible at the deeper depths.

Pavement
The paved measurement points (MP06 and MP07) generally show a strong correlation, except at 300mm depth. At deeper levels, 600mm and 1000mm, correlation weakens but remains sufficient. This change can be attributed to two factors.

First, measurement accuracy is affected by the low soil moisture content. Early in the study, the access tube at MP06 was no longer air-tight, and a similar issue later occurred at MP07, impacting data consistency. Second, differences in soil texture between these points contribute to variations in moisture dynamics, Table 3.1.

Interrelations with other measurement points are also observed in Figure 3.2. At shallow depths of 100mm and 200mm, the moderate to strong correlations may result from small gaps around the access tube, allowing limited precipitation to enter the soil. This effect is visible in Figure 3.1a, as the paved measurement points show similar soil moisture dynamics as the other green measurement points at these depths. At greater depths, observed correlations are likely due to minimal soil moisture dynamics, an observation at multiple measurement points (Figure 3.1d and Figure 3.1e).

Trees
The measurement points near trees (MP09 and MP10) show a strong correlation at 100mm and a moderate correlation at 300mm. However, at deeper measurement levels, no significant correlation is observed. Several factors contribute to these interrelations.

First, tree species differences play a key role. Each measurement point is located under a different tree species, as illustrated in Figure 3.3), leading to variations in canopy structure that influence the amount of precipitation and solar radiation reaching the soil (Tanaka & Hashimoto, 2006). Additionally, differences in root system architecture affect soil moisture dynamics, with variation in root depth and distribution shaping how water is absorbed and retained (Tanaka & Hashimoto, 2006). These species-specific characteristics introduce additional variability, particularly at greater depths.

Interestingly, the measurement points near trees also exhibit correlations with shaded grass-covered areas (MP01 and MP05), where moderate to strong correlation persists up to 300mm. This suggests that shading, whether from trees or buildings, has a comparable effect on soil moisture dynamics at shallower depths. However, at greater depths, the influence of trees becomes more distinct due to the active role of their root system, whereas buildings lack this subsurface interaction. While both trees and buildings modify microclimatic conditions by reducing direct solar radiation, only trees directly alter soil moisture distribution through root water uptake.

The interrelations between measurement points highlight how urban environmental conditions influence soil moisture dynamics. Grass-covered areas show strong correlations up to 300mm, but deeper layers are affected by sun exposure and groundwater uplift. Paved areas show limited moisture dynamics,

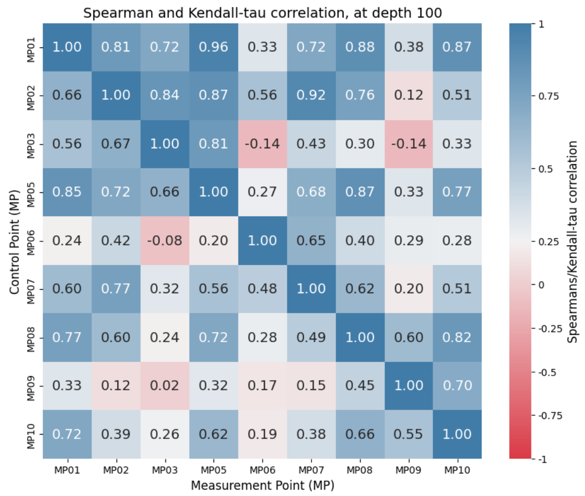

(a) Depth of 100mm

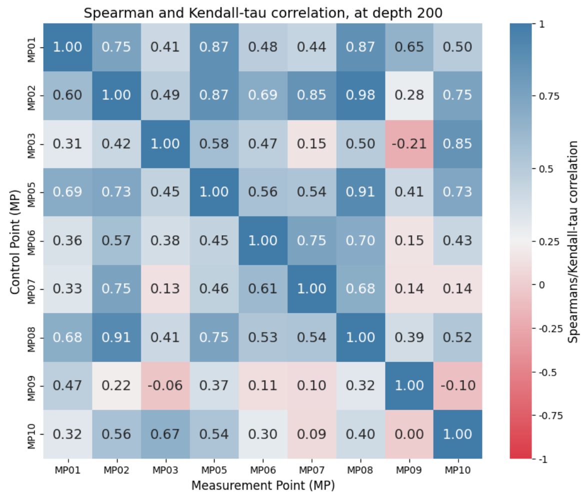

(b) Depth of 200mm

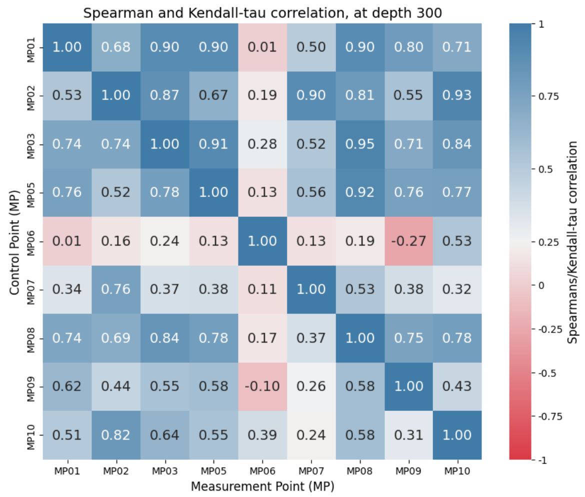

(c) Depth of 300mm

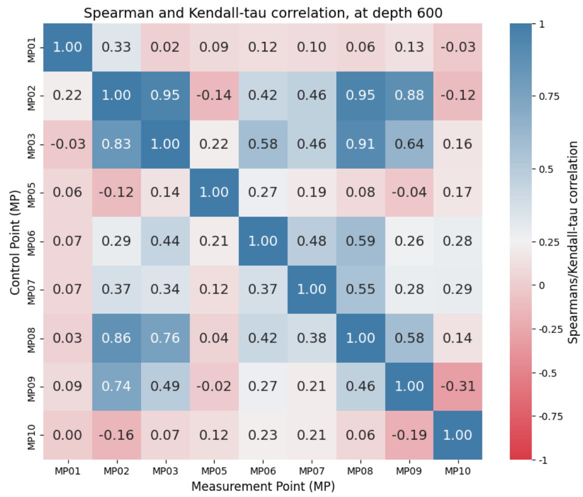

(d) Depth of 600mm

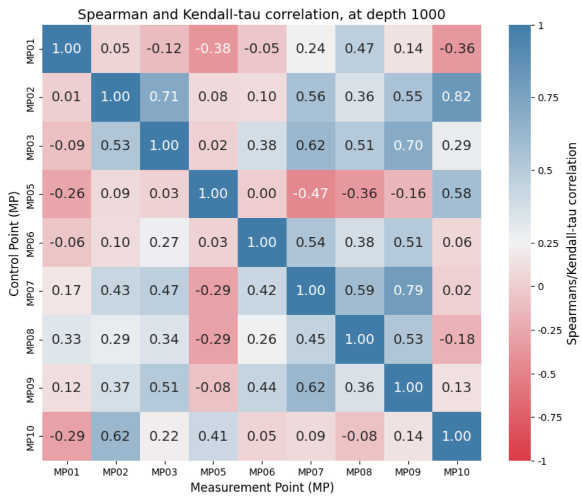

(e) Depth of 1000mm

Figure 3.2: The correlation between the measurement points per depth, visualised in a heatmap. The bottom left triangle is for Kendall's correlation τ_b and the upper right triangle is for Spearman's correlation r_s. A darker blue color indicates a strong correlation, which fades to light blue, moderate to weak correlation. A white or red colour indicates a poor correlation between the measurement points.

(a) The canopy of the tree at MP09

(b) The canopy of the tree at MP10

Figure 3.3: The canopy of the trees at MP09 and MP10 straight above the measurement points.

maintaining strong correlations at most depths except at 300mm, where low soil moisture content, air-tight access tube placement, and soil texture differences likely contribute to variations. Tree-covered areas show correlation at shallower depths, 100mm to 300mm, but species-specific canopy and root characteristics introduce variability at deeper levels. Notably, the shading effects of trees and buildings similarly impact upper soil layers, though tree roots create distinct moisture patterns at greater depths. These findings underscore the complex interactions between vegetation, shading, and soil properties in urban environments.

While urban environmental conditions significantly influence soil moisture dynamics, another major influence is soil texture. Soil texture varies across measurement points and affects water retention and movement, particularly at deeper depths. The next section examines these variations in soil texture and their relationship to soil moisture dynamics.

3.2. Soil Texture

Soil moisture dynamics are influenced by both urban environmental conditions and soil textures. This section examines the similarities in soil texture across measurement points and their correlation with soil moisture dynamics. The discussion follows a top-to-bottom approach, with the soil textures for each measurement point summarized in Table 3.1.

At shallower depths, 15–20cm and 30-35cm, the soil textures among green measurement points are largely similar, with a few exceptions. At 15–20cm, all green measurement points share the same soil texture except MP05. This consistency is expected, as the organic layer remains relatively uniform. Among paved measurement points (MP06 and MP07), a similarity in soil texture is observed, but only at this specific depth. At 30–35cm, MP01 stands out as different from the other green measurement points, while MP01 and MP05, both located in grass-covered and shaded areas, show no soil texture similarities. Since no distinct new patterns emerged at these depths, no additional groupings were analyzed. The implications of these findings are further explored in Section 3.1.2, categorised by urban environmental conditions.

As depth increases, variations in soil texture become more pronounced, and clear patterns are less

Table 3.1: The soil textures for all measurement points

Depth [cm]	MP01			MP02			MP03		
	Sand (%)	Silt (%)	Clay (%)	Sand (%)	Silt (%)	Clay (%)	Sand (%)	Silt (%)	Clay (%)
15-20	16	68	15	12	74	13	14	72	14
30-35	29	55	16	15	72	13	19	69	12
45-50	24	48	27	21	58	18	14	80	5
75-80	33	45	21	2	92	6	18	77	5

Depth [cm]	MP05			MP06			MP07		
	Sand (%)	Silt (%)	Clay (%)	Sand (%)	Silt (%)	Clay (%)	Sand (%)	Silt (%)	Clay (%)
15-20	36	59	6	19	75	6	12	82	7
30-35	22	72	6	66	34	0	8	50	41
45-50	3	95	2	56	36	9	17	80	3
75-80	3	95	2	12	83	5	29	47	23

Depth [cm]	MP08			MP09			MP10		
	Sand (%)	Silt (%)	Clay (%)	Sand (%)	Silt (%)	Clay (%)	Sand (%)	Silt (%)	Clay (%)
15-20	13	73	14	15	68	16	23	66	11
30-35	18	71	11	16	69	13	20	72	9
45-50	15	79	6	27	62	9	40	47	12
75-80	17	78	5	29	62	8	29	46	25

Note: MP04 is excluded from the analysis due to measurement disruptions.

evident. At 450–500mm, two sets of measurement points, MP02 with MP09 and MP03 with MP07, exhibit similar soil textures. By 75–80cm, three distinct groups emerge: 1) MP01, MP07, and MP10; 2) MP02 and MP05; and 3) MP03, MP06, and MP08. These groupings suggest that deeper soil layers display more variation compared to shallower depths.

The observed variations in soil texture at greater depths result in different levels of correlation, ranging from strong to weak, among the measurement points. This indicates that while soil texture plays a role in soil moisture dynamics, it is not the only factor when considered independently of urban environmental conditions.

While soil texture influences soil moisture dynamics, it is not the sole determining factor. To further analyse these dynamics, HYDRUS-1D is used to model the impact of drought conditions. The next section evaluates the model's performance before applying drought scenarios to grass-covered areas.

3.3. HYDRUS-1D

HYDRUS-1D is used to model the impact of drought on soil moisture dynamics in urban areas. Before applying the 2018 drought scenario, the model's performance is evaluated under the weather conditions of the measurement period. The drought analysis focuses on grass-covered areas, as initial findings indicate that paved areas are not relevant. Measurement points with trees exhibited poor model performance and are therefore excluded from the analysis. This section focuses on the model performance for each measurement.

3.3.1. Model performance

The model performance is determined by its settings, input parameters and the optimization of the soil hydraulic parameters. The model settings are bounded by the available options and 1D water flows. The model settings assume vertical flow, which is the main flow component in unsaturated conditions, but some horizontal flow is considered as well, as it plays a role in saturated conditions.

The input parameters for the model are derived from meteorological data collected from a weather station located 500m from the study area. While these parameters provide a realistic representation of weather conditions, differences exist between the study site and the station due to urban factors such as the heat island effect and wind blockage by buildings. Variables such as wind speed, solar radiation, and temperature, which are integral in the Penman-Monteith equation, may introduce discrepancies between modelled and measured soil moisture dynamics. For instance, shaded areas receive direct sunlight until approximately 14:00, after which buildings cast shadows. This variation in solar exposure, though accounted for in the model, may still contribute to deviations in performance.

The model is optimized for five grass measurement points (MP01, MP02, MP03, MP05 and MP08) by selecting site-specific hydraulic parameters, detailed in Section 2.3.4. The optimization process is constrained by the model's ability to maintain a stable water balance (Ouédraogo et al., 2025). The parameters optimized are α, n, and K_s, with α and n significantly influencing performance and K_s playing a crucial role in drainage (Ouédraogo et al., 2025). Given that only 33 measurement points are available, the model is fitted to a limited dataset, which may impact its accuracy.

Model performance is assessed using Kendall's, τ_b, and Spearman's, r_s, correlations, as explained in Section 2.3.6. At depths of 100mm, 200mm, and 300mm, the model meets the correlation threshold of $\tau_b/r_s \geq 0.4$. However, performance declines at 600mm and 1000mm, likely due to groundwater interactions, which are not accounted for in the model. These discrepancies lead to differences between the modelled and measured soil moisture dynamics.

The following sections provide a detailed evaluation of the model's performance at each measurement point, with visual comparisons of measured and modelled soil moisture dynamics. Differences in scale between the two datasets, explained in Section 2.3.6, are addressed by plotting them on separate axes.

MP01: Shaded area
The model performance results for MP01 are in Figure 3.4 and show a strong correlation at 100mm, 200mm and 300mm, but a weak or nonexistent correlation at 600mm and 1000mm. This decline in performance is likely due to groundwater interactions and the presence of a tree located 30m away. The lack of model performance at 1000mm is attributed to the threshold value for the standard deviation of $1E-5$, not being met, which resulted in the calculation being skipped. Additionally, the model's underperformance at 600mm and the absence of soil moisture dynamics at 1000mm make these depths unsuitable for further drought analysis. Despite these limitations, the model effectively captures soil moisture dynamics at shallow depths, responding well to weather conditions. Therefore, further analysis will focus on depths up to 300mm, where the model has a reliable performance.

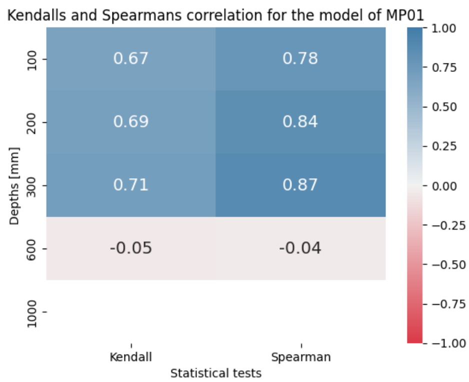

(a) Model performance of MP01.

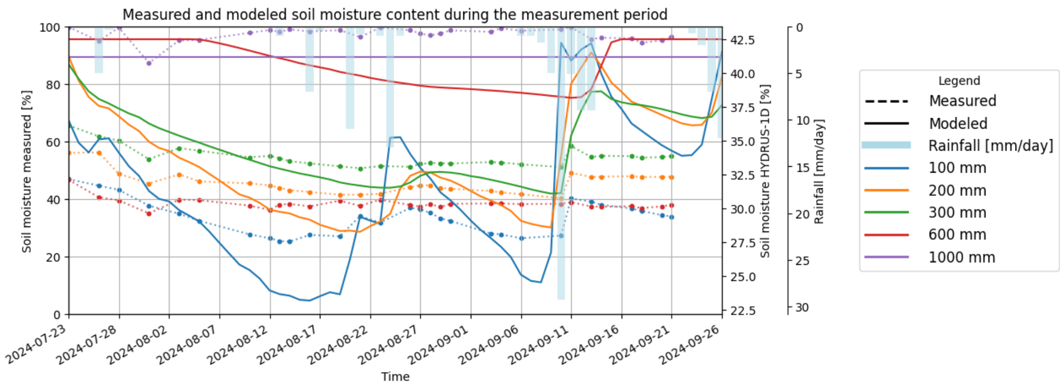

(b) Observed and modelled soil moisture content for MP01.

Figure 3.4: Model performance of MP01 relative to measured soil moisture content. The heatmap (a) shows Kendall's and Spearman's correlation and the bottom figure (b) illustrates soil moisture dynamics.

MP02: Sunny area

MP02 exhibits the best model performance across all depths, shown in Figure 3.5. This can be related to the shorter measurement period, as data collection stopped on September 5th due to damage to the access tube and measurements were no longer possible. Consequently, the major precipitation event on September 10th, which could have affected the correlation, is not included in the dataset. Despite this limitation, MP02 is retained for further analysis as the model recognises the weather patterns.

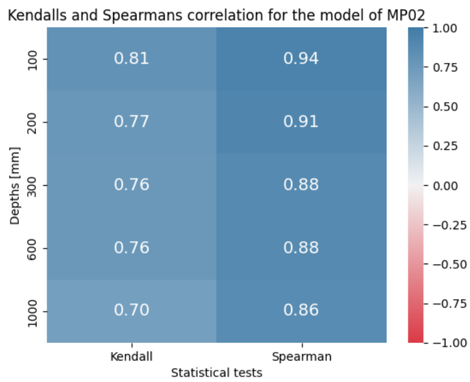

(a) Model performance of MP02.

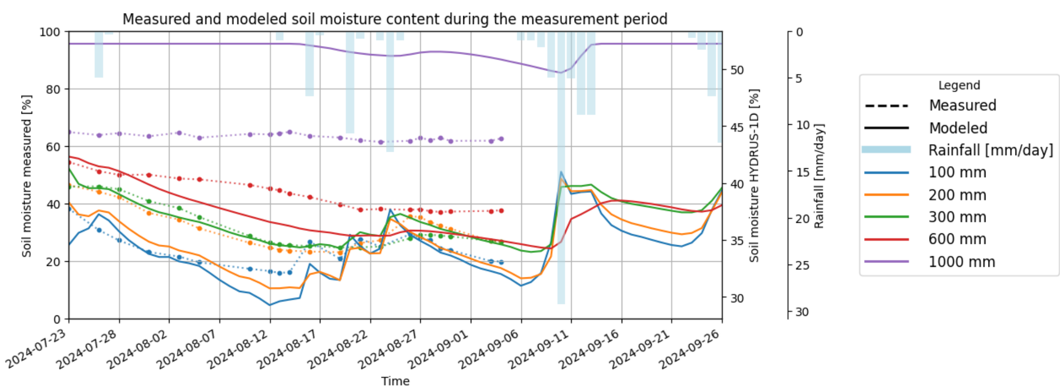

(b) Observed and modelled soil moisture content for MP02.

Figure 3.5: Model performance of MP02 relative to measured soil moisture content. The heatmap (a) shows Kendall's and Spearman's correlation and the bottom figure (b) illustrates soil moisture dynamics.

MP03: Sunny area

MP03 meets the model performance criteria for all depths, as depicted in Figure 3.6. A minor air gap between the top part of the access tube and the soil, present from an early stage in the measurement period, may have influenced the results. Nevertheless, the modelled soil moisture dynamics align well with measured values.

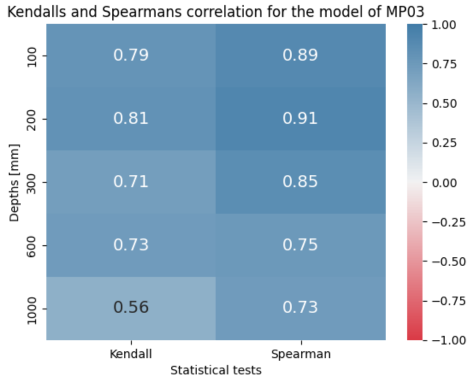

(a) Model performance of MP03.

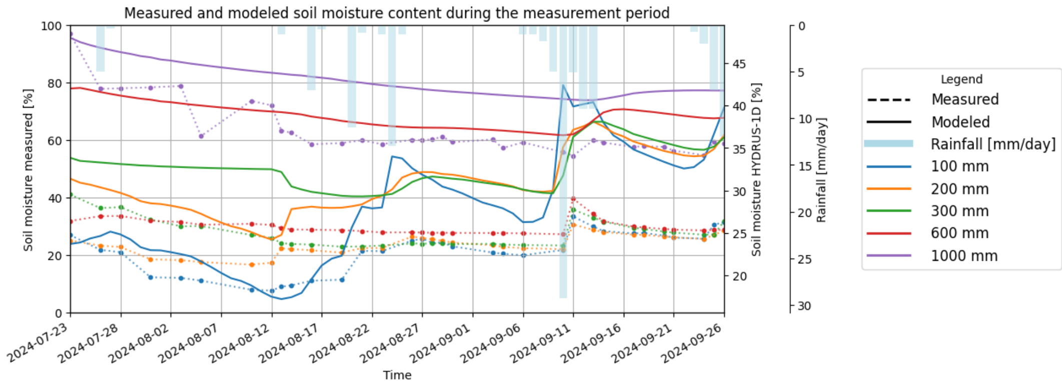

(b) Observed and modelled soil moisture content for MP03.

Figure 3.6: Model performance of MP03 relative to measured soil moisture content. The heatmap (a) shows Kendall's and Spearman's correlation and the bottom figure (b) illustrates soil moisture dynamics.

MP05: Shaded area

MP05 meets the performance threshold at all depths except 600mm, as shown in Figure 3.7. While some correlation exists at this depth, it is weak, and the reason for this underperformance remains unclear and may be attributed to measurement error. At both 600mm and 1000mm, the modelled soil moisture values are consistently higher than the measured values, despite differences in scale, as explained in Section 2.3.6. The model tends to simulate near-saturation conditions at these depths, whereas the measured values indicate lower soil moisture levels. When using this model for drought analysis, these observations at greater depths should be considered before drawing conclusions.

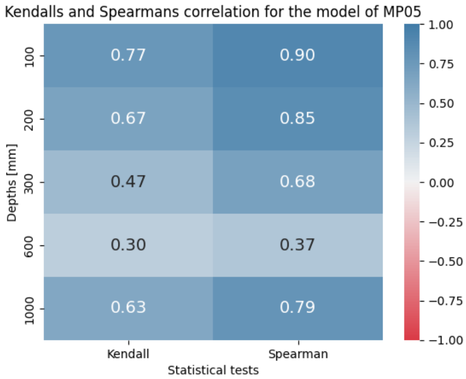

(a) Model performance of MP05.

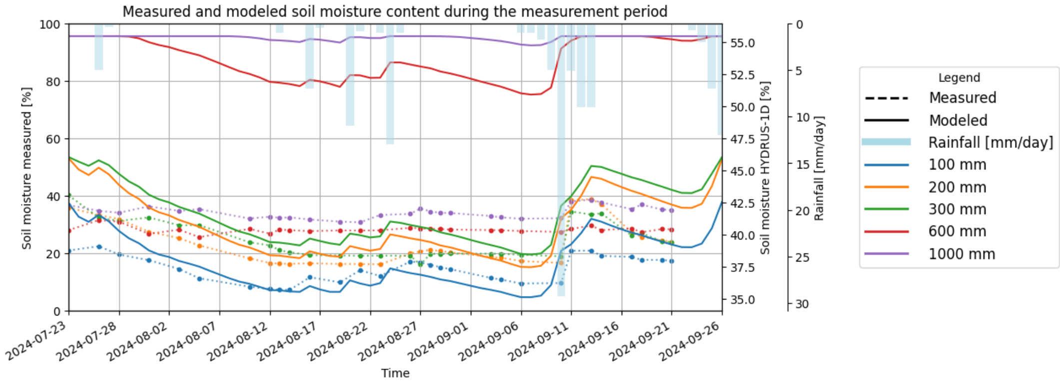

(b) Observed and modelled soil moisture content for MP05.

Figure 3.7: Model performance of MP05 relative to measured soil moisture content. The heatmap (a) shows Kendall's and Spearman's correlation and the bottom figure (b) illustrates soil moisture dynamics.

MP08: Sunny area

MP08 shows a strong model correlation at all depths except 1000mm, where a negative correlation is observed, Figure 3.8. This discrepancy can be attributed to groundwater effects, leading to the exclusion of the 1000mm depth from further analysis. A deviation in soil moisture trends occurred after September 21st due to damage to the access tube by a lawnmower.

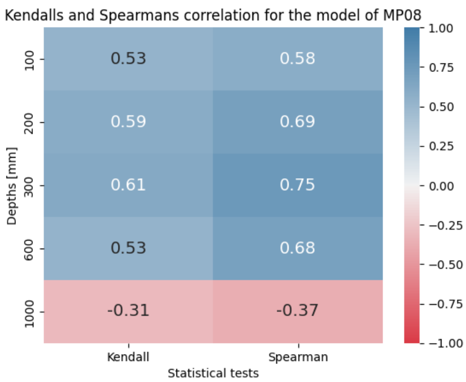

(a) Model performance of MP08.

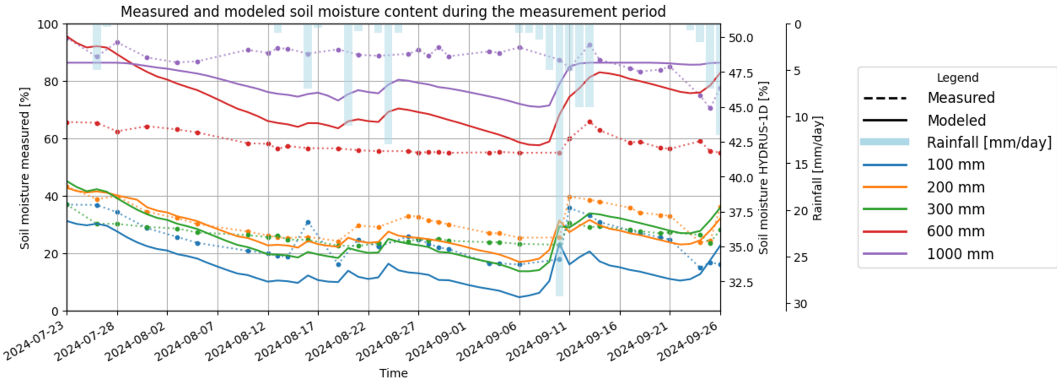

(b) Observed and modelled soil moisture content for MP08.

Figure 3.8: Model performance of MP08 relative to measured soil moisture content. The heatmap (a) shows Kendall's and Spearman's correlation and the bottom figure (b) illustrates soil moisture dynamics.

The model's performance varies across measurement points and depths, with strong correlation observed at shallower depths, 100mm to 300mm, but weaker performance at greater depths due to groundwater interactions. Additionally, differences in meteorological conditions between the study site and the weather station introduce minor discrepancies in soil moisture predictions.

After assessing the model's performance and the factors influencing its accuracy, the next step is to apply it to a specific climatic event: the 2018 drought. This scenario provides valuable insights into soil moisture dynamics during prolonged dry periods. The analysis examines differences in environmental conditions, comparing sunny and shaded measurement points, while also considering the impact of extreme initial soil moisture conditions on drought development to evaluate their respective responses to drought stress.

3.4. Drought of 2018

The drought of 2018 serves as a case study to model and assess its impact on soil moisture dynamics at grass-covered measurement points (MP01, MP02, MP03, MP05, and MP08). Given the urban environmental conditions, the analysis distinguishes between sunny locations (MP02, MP03, and MP08) and shaded locations (MP01 and MP05). The focus is on identifying drought patterns within these two classifications and understanding the role of environmental conditions on soil moisture retention and depletion.

Additionally, to better understand the effect of pre-drought conditions, the influence of initial soil moisture levels was examined by comparing dry and wet starting conditions. These extreme scenarios help assess how soil moisture evolves under different initial conditions within the model and how they interact with urban environmental factors.

3.4.1. Soil moisture dynamics

The overall modelled soil moisture trends during the 2018 drought align well with the measured dynamics, considering urban environmental conditions only. Shaded areas tend to retain water longer during prolonged dry periods, whereas sunny locations experience more rapid depletion. This confirms that the urban environmental conditions, the sun and shadow, significantly influence the soil moisture behaviour. These observations are based on the visualisation in Figure 3.9.

The meteorological differences in the measurement period and the drought of 2018 are significant. While differences in sample size may play a role, the drying patterns observed across all depths are different. In the shallow layers, 100mm and 200mm, soil moisture values rapidly decline to critically low soil moisture levels close to 0%. This trend is visible across all depths, but a clear distinction emerges between the upper layers, 100mm and 200mm, and the deeper layers, 300mm and beyond.

At depths of up to 200mm, soil moisture shows an active response to meteorological conditions in both scenarios. However, during dry spells in 2018, the decrease in soil moisture is more pronounced compared to the measurement period, suggesting stronger evaporation. During and after precipitation events, soil moisture levels increase across all depths. However, while these increases are evident down to 300mm during the measurement period, during the 2018 drought, they are primarily observed in the top 200mm.

A comparison of soil moisture behavior at depths of 300mm and beyond reveals the deeper impact of drought conditions. The gradual decline in soil moisture at these depths suggests a lowering of the groundwater table, signaling the onset of hydrological drought (Dabrowska et al., 2023). Furthermore, the extreme precipitation deficit reported by KNMI (2024), combined with the agricultural drought observed in the upper soil layers, indicates that all components of urban drought are present.

Effects of sun
At the sunny locations (MP02, MP03 and MP08), soil moisture values decrease consistently across all depths. Among these sites, MP02 exhibits higher soil moisture contents compared to MP03 and MP08, likely due to differences in soil texture, Table 3.1. Despite these variations, the overall soil moisture dynamics at MP02 follow a similar pattern to the other sunny locations.

Before the onset of the dry spell in June, precipitation influences soil moisture across all depths, with clear responses visible in the dynamics. However, after the extended drought period, particularly by late July, this response changes. At depths of up to 300mm, precipitation events continue to create a noticeable peak in soil moisture. In contrast, at 600mm and 1000mm, precipitation does not directly increase soil moisture content, instead, changes in decay rates suggest a more gradual response to soil moisture availability.

Effects of shadow
The shaded measurement points (MP01 and MP05), soil moisture trends generally follow those observed in sunny measurement points. Notably, shaded measurement points retain soil moisture longer, particularly at depths of 300mm and beyond. This highlights the capacity of shaded environments to buffer against extreme drying.

At MP01, the most pronounced soil moisture increase following precipitation is observed at 100mm depth, with occasional responses at 200mm. In contrast, MP05 exhibits more widespread responses, with precipitation effects visible down to 300mm and, to a lesser extent, at greater depths. These differences in soil moisture behaviour are likely due to variations in soil texture between the two shaded locations, Table 3.1. However, at depths of 600mm and 1000mm, the model at MP05 is leading in soil moisture dynamics, explained in Section 3.3.1. It shows a decrease in soil moisture during the dry spell, but the values tend to be higher compared to the sunny measurement points.

When comparing soil moisture dynamics between sunny and shaded areas, both show that the upper layers, 100mm and 200mm, reach critically low moisture levels at similar rates. Additionally, the recovery in response to precipitation in August follows a similar pattern at 100mm and 200mm across all locations. However, from 300mm downward, differences in response emerge. These variations cannot be solely attributed to sun exposure but are more likely influenced by soil texture.

For instance, at 300mm, MP01 exhibits barely any response to precipitation, while MP05 shows a strong reaction. This contrast can be explained by soil textures, MP01 contains a mix of sand, silt and clay, while MP05 consists primarily of silt, which retains moisture more effectively. At greater depths, 600mm and 1000mm, soil moisture declines during the drought and stabilizes once precipitation resumes in August, a trend observed in both sunny and shaded areas. Overall, while sun exposure influences soil moisture dynamics during drought, soil texture appears to play a more dominant role at greater depths, as also noted by N. Li et al. (2024).

These results highlight the influence of sun exposure and soil texture on soil moisture dynamics during drought. However, another critical factor influencing soil moisture response is the initial soil moisture condition.

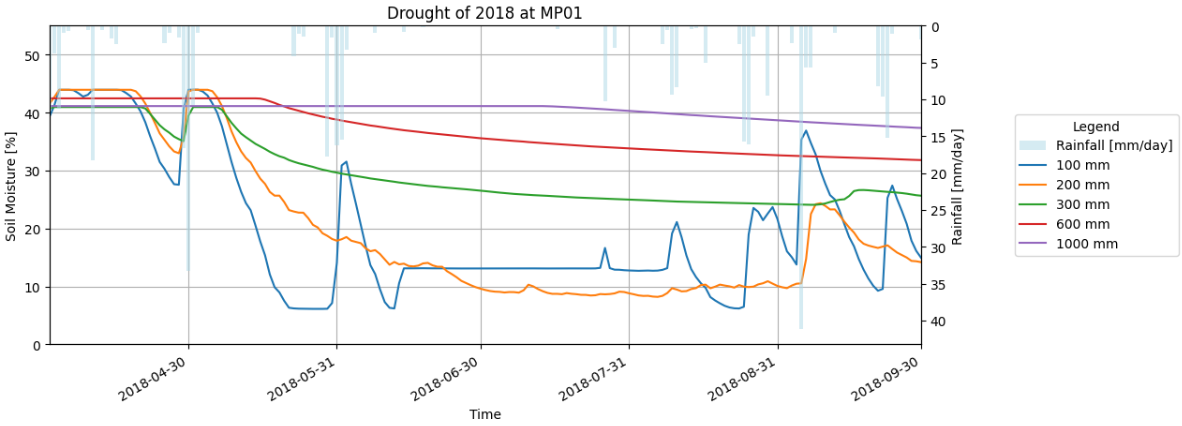

(a) MP01

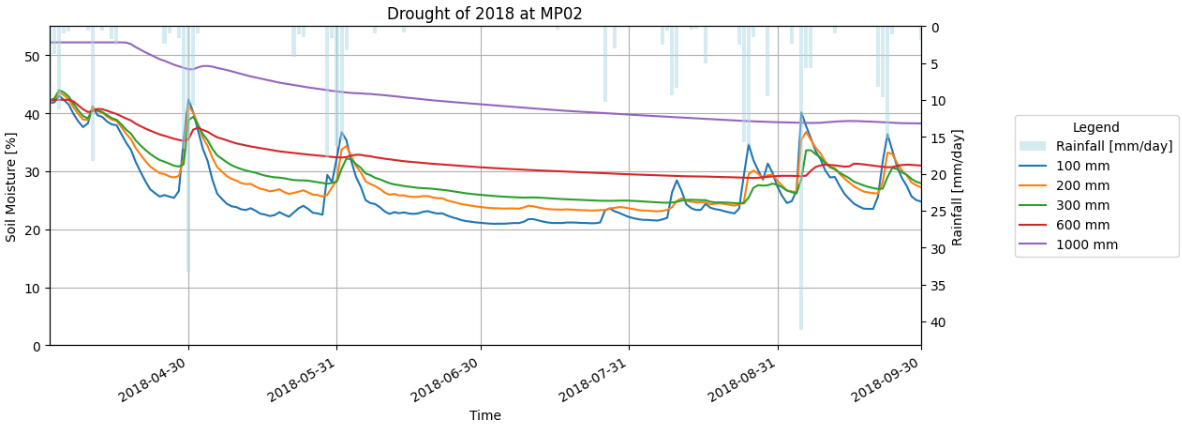

(b) MP02

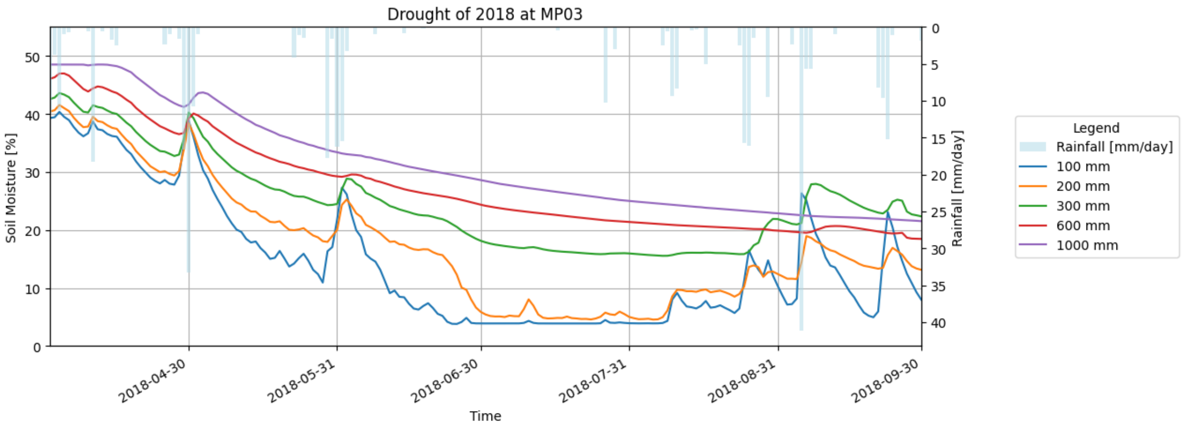

(c) MP03

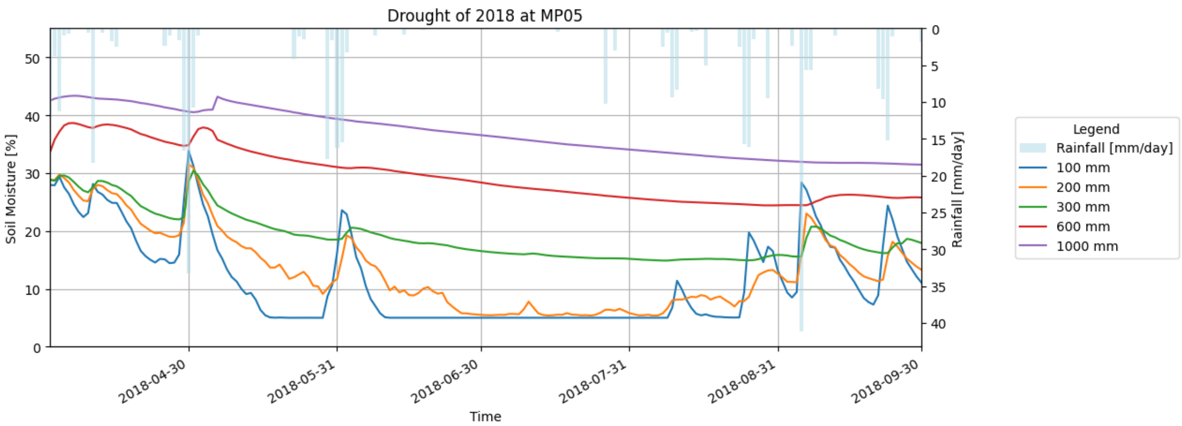

(d) MP05

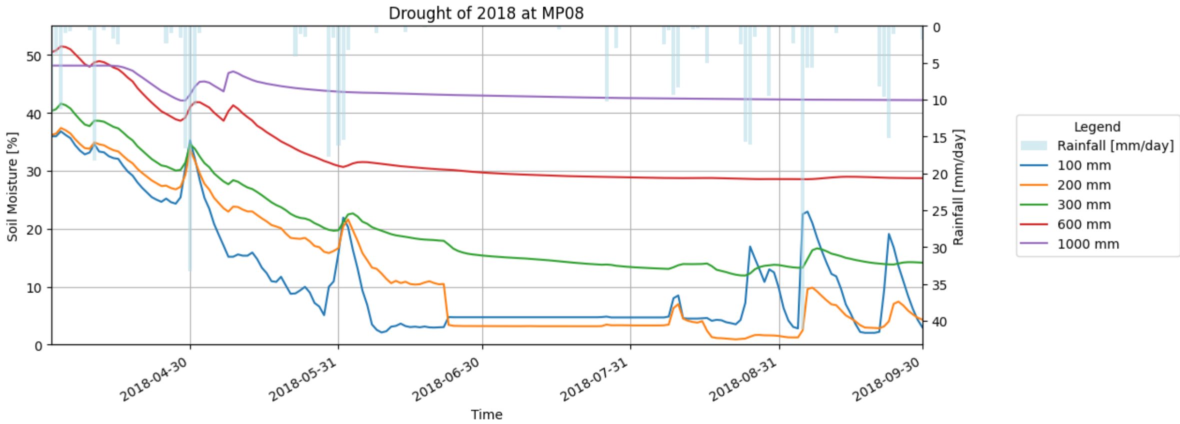

(e) MP08

Figure 3.9: The soil moisture dynamcis for five depths at measurement points MP01, MP02, MP03, MP05 and MP08, where the drought of 2018 is considered.

3.4.2. Effects of initial soil moisture conditions

To evaluate the influence of pre-drought soil moisture levels on drying patterns, the initial soil moisture conditions were adjusted to represent extreme scenarios, either extremely dry or wet. These conditions were applied to the drought of 2018, as explained in Section 2.3.5. The resulting soil moisture responses for each measurement point are visualized in Figure 3.10. In the figures, dry initial conditions are represented by dashed lines, while wet conditions are shown as continuous lines.

At shallow depths, 100mm to 200mm, soil moisture responds actively to precipitation, with stronger depletion during drought conditions. At greater depths, 300mm and beyond, soil moisture dynamics indicate the onset of hydrological drought, with groundwater levels likely decreasing in response to prolonged dry conditions.

Below 200mm depth, the impact of initial moisture conditions becomes more pronounced, with steeper declines under wet initial soil conditions. his pattern suggests that higher initial moisture levels provide more water for evaporation and root uptake, leading to a faster decline once the drought begins. In deeper layers, these differences persist longer in shaded locations, where soil moisture retention is higher. In contrast, in sun-exposed areas, both wet and dry initial conditions result in similar moisture levels by the end of the drought.

The influence of initial conditions varies across measurement points, except for MP02, where differences are minimal, depicted in Figure 3.10b. At 100mm depth, soil moisture behaves similarly under both dry and wet initial conditions. Although the wet scenario initially exhibits higher moisture content, the difference diminishes quickly once the dry spell begins. In contrast, MP05, illustrated in Figure 3.10d, shows a more prolonged divergence, with the wet initial condition maintaining higher soil moisture levels for a longer period before converging with the dry condition.

A key observation is that soil moisture dynamics at 100mm are largely independent of initial conditions. This suggests that root water uptake plays a role in buffering against extreme initial wet and dry soil moisture conditions, as shallow-rooted vegetation extracts moisture at similar rates regardless of initial soil moisture content. This aligns with findings from previous studies highlighting root depth as a key component in soil-water balance modelling (Z. Li et al., 2019).

These results confirm that urban environmental factors, particularly sun exposure and shading, significantly influence soil moisture dynamics during drought. Shaded areas retain moisture longer, whereas sun-exposed locations experience more rapid depletion. Additionally, differences in drying patterns between the 2018 drought and the measurement period highlight the variability in soil moisture responses under different meteorological conditions.

While these findings offer valuable insights, it is important to acknowledge that the effects of extreme initial soil moisture conditions are influenced by their implementation in HYDRUS-1D. The initial moisture profiles were adjusted to ensure model convergence and a closed water balance, meaning that absolute values serve as estimations rather than exact field representations. Nonetheless, the results underscore the critical role of initial soil moisture conditions in shaping soil moisture depletion during drought.

The analysis of extreme initial moisture conditions further reinforces these findings, demonstrating that initial soil moisture levels impact drying rates but ultimately converge under prolonged drought stress. While model limitations introduce some uncertainty, these results provide a valuable framework for understanding urban drought dynamics and improving soil moisture predictions under different environmental conditions.

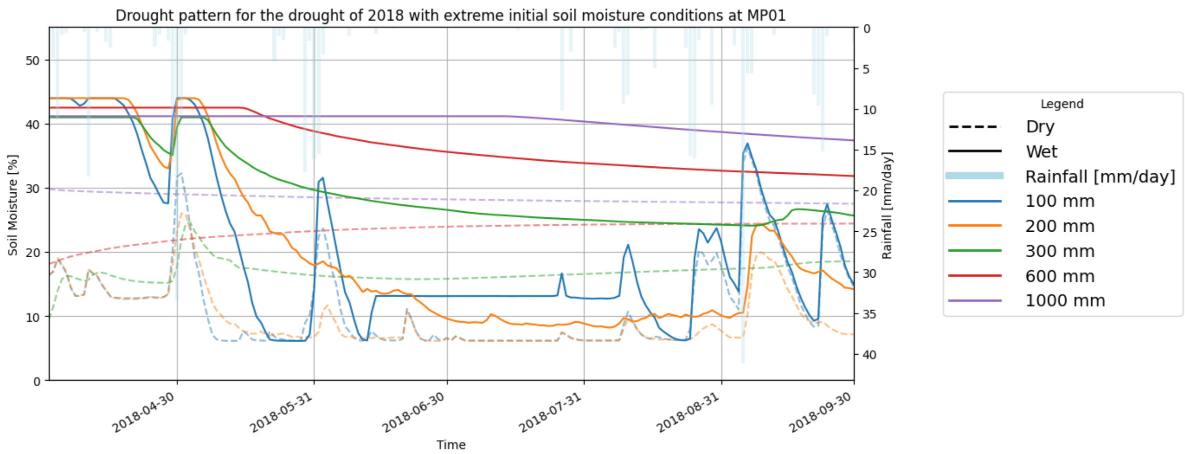

(a) MP01m

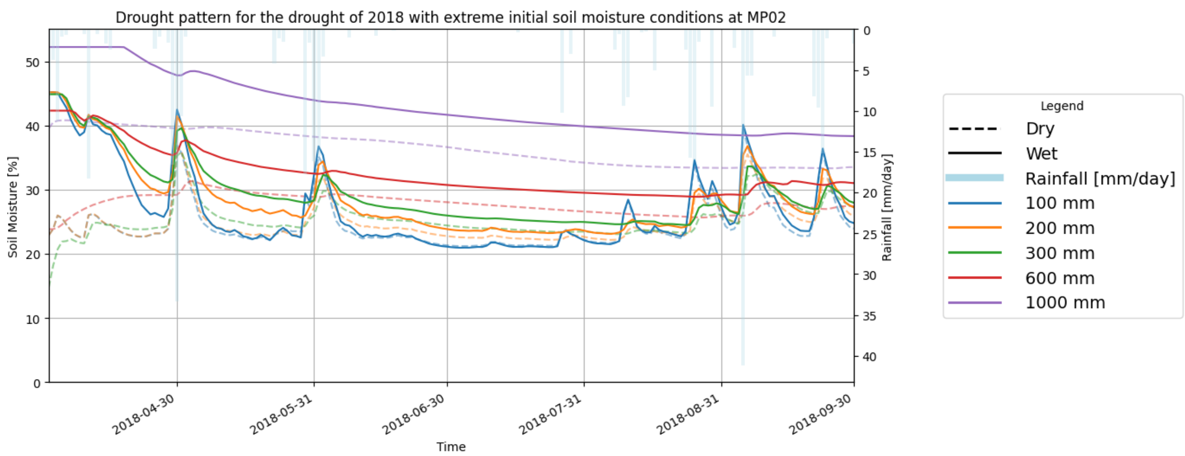

(b) MP02

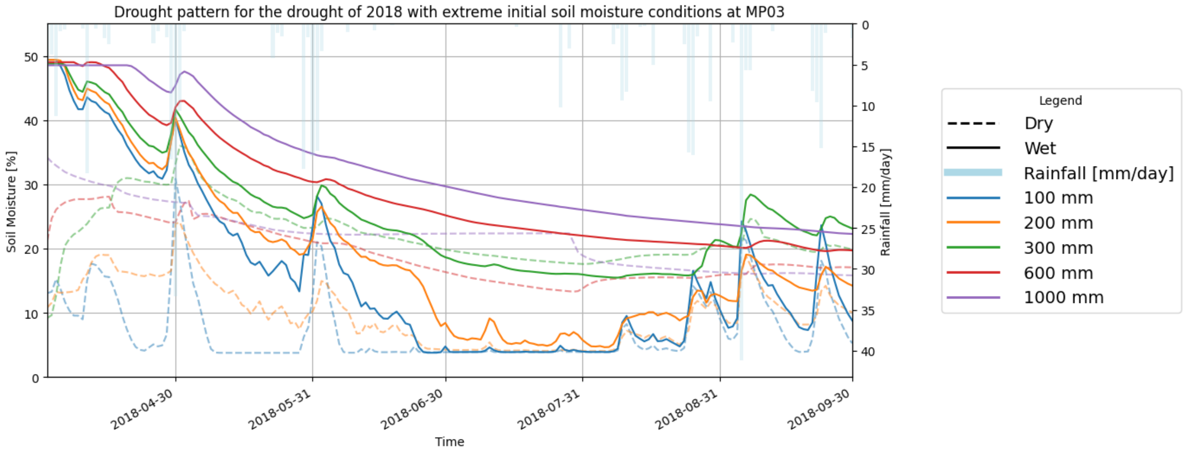

(c) MP03

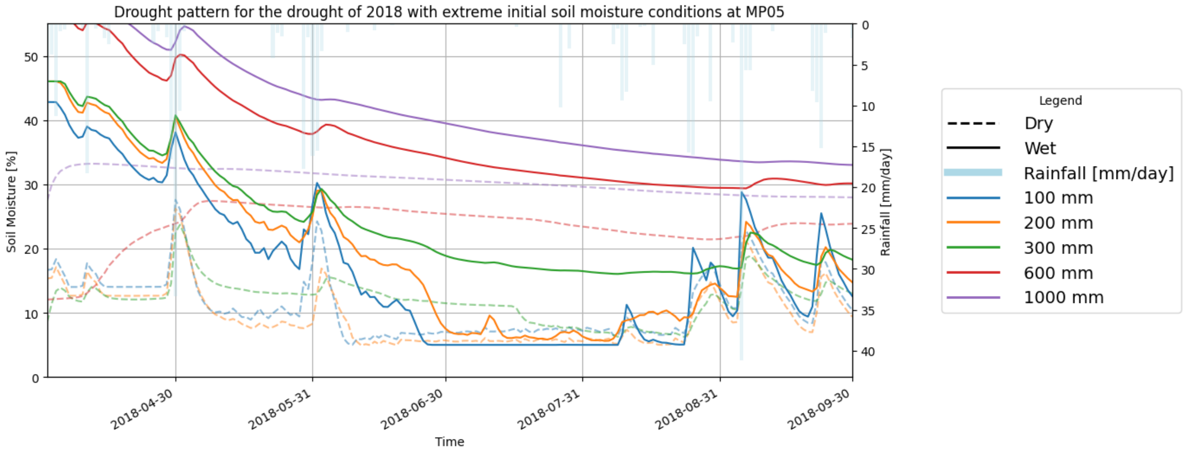

(d) MP05

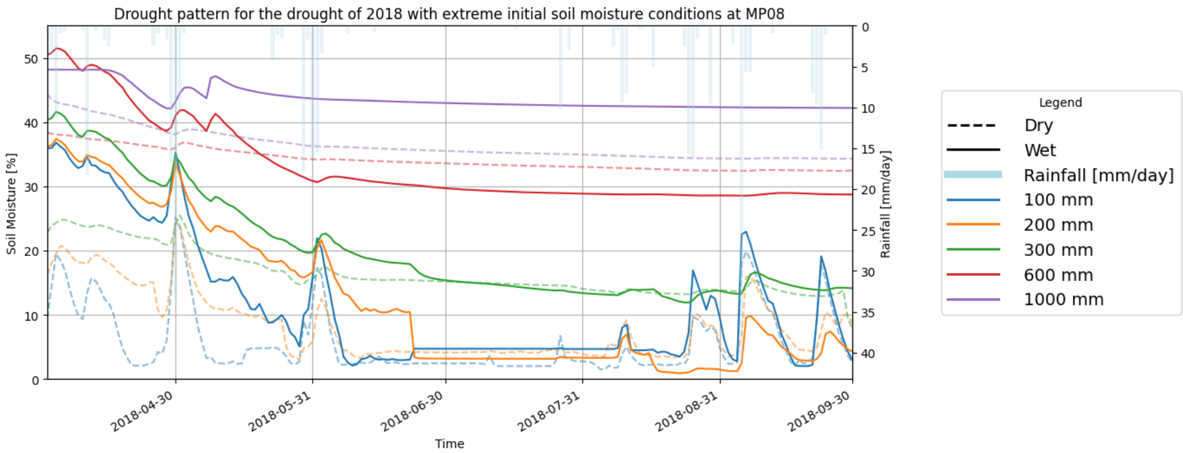

(e) MP08

Figure 3.10: The effect of extremely dry and wet initial soil moisture conditions on the drought pattern for MP01, MP02, MP03, MP05 and MP08.

4 Discussion

Understanding soil moisture dynamics is essential for assessing urban drought impacts, as soil moisture directly influences vegetation health, water availability, and overall ecosystem stability. Soil moisture levels are governed by complex interactions between meteorological circumstances, soil textures, and vegetation types.

This study explored how these factors influence soil moisture during drought, using measured soil moisture data and the drought of 2018 as a case study. The findings highlight the interplay between meteorological conditions, soil texture, and urban environmental conditions in shaping soil-water balance. This discussion connects the results to existing literature, focusing on urban drought, environmental conditions, and key parameters of the soil-water balance. Finally, the study's limitations are addressed.

4.1. Urban drought

The results confirm that urban drought is a multi-dimensional phenomenon influenced by various environmental and hydrological processes. Understanding the different types of drought, meteorological, agricultural, hydrological and socioeconomic (Dabrowska et al., 2023; Keyantash, 2021), is crucial to interpreting the observed soil moisture dynamics.

Meteorological drought, characterized by prolonged periods of low precipitation, directly leads to soil moisture deficits. This was evident during the 2018 drought, where the modelled soil moisture content declined for all measurement points. The observed reduction in shallow and deeper soil moisture highlights the direct impact of meteorological drought on soil moisture availability. A similar observation at the shallow depths is visible in the measured soil moisture dynamics.

Agricultural drought was reflected in the rapid depletion of soil moisture at shallow depths, at 100mm to 300mm, where plant roots primarily extract water. Both measured soil moisture contents and the modelled drought of 2018 illustrate this phenomenon, as moisture levels at these depths decline, regardless of sun exposure. The modelled soil moisture values even show critical low values. In deeper soil layers, from 300mm and beyond, the decline in soil moisture suggests a transition toward hydrological drought. Soil moisture reductions at 600mm and 1000mm indicate diminished groundwater recharge, supporting existing studies that link prolonged dry conditions to significant groundwater depletion. These findings reinforce the notion that urban drought involves multiple interacting drought types, with meteorological drought triggering both agricultural and hydrological drought effects (Bartholomeus et al., 2023; Dabrowska et al., 2023; Keyantash, 2021; Yimer et al., 2024; X. Zhang et al., 2019).

4.2. Urban environmental conditions

The study highlights the significant role of five urban environmental conditions: sun, shadow, grass, trees and pavement. The discussion is categorised based on the urban environmental conditions, as each influences soil moisture dynamics differently: grass (sun and shadow), pavement and trees.

Grass
Measurement points in sunny locations exhibited rapid soil moisture depletion, particularly in the upper 200mm to 300mm. Increased solar radiation and higher temperatures in these areas accelerate evaporation, reducing soil moisture availability, as predicted by the Penman-Monteith and soil-water balance equations.

In contrast, shaded areas retained soil moisture for longer periods due to reduced solar radiation, which lowers evaporation rates. This finding underscores the role of urban green infrastructure, such as tree canopies and shaded parks, in mitigating drought impacts by preserving soil moisture.

Pavement
Urban environments often contain impermeable surfaces such as roads and pavements, reducing subsurface moisture recharge. The study suggests that these areas exhibit higher surface runoff, leading to distinct soil moisture retention characteristics compared to permeable surfaces.

Trees
Measurement points under tree canopies showed significant differences in soil moisture depletion patterns. The shading provided by the tree canopy reduced direct solar radiation, which lowered evaporation rates and helped retain soil moisture. Additionally, root water uptake emerged as a key driver of moisture loss, especially in the upper soil layers. Trees with deeper root systems were able to access moisture from lower depths, offering greater resilience against prolonged dry conditions. Thus, trees play a dual role: they mitigate drought effects through shading and actively extract moisture from deeper soil layers. This dual influence highlights the complex contribution of trees to urban soil moisture dynamics and points to the need for further research to fully understand their impact.

4.3. Soil-water balance

This section examines the key components of the soil-water balance, focusing on precipitation and evaporation as primary fluxes, the role of root water uptake, and the influence of soil texture on moisture retention. Additionally, it highlights the importance of incorporating groundwater dynamics unto urban drought assessments for a more comprehensive understanding of long-term moisture fluctuations.

The two primary fluxes governing soil moisture dynamics in the soil-water balance equation are precipitation, P, which replenishes soil moisture, and evaporation, ET, which depletes it (Z. Li et al., 2019). Evaporation is estimated using the Penman-Monteith equation (Allen et al., 1998; Daly & Porporato, 2006).

The evaporation process is particularly pronounced in sunny areas, where higher temperatures and direct solar radiation (Brown, 2000) caused a more rapid depletion of surface soil moisture, by an increased ET. Conversely, shaded areas showed greater moisture retention, reinforcing the importance of reduced evaporation rates in mitigating drought effects. The evaporation process consists of both soil evaporation and transpiration. In sunny areas, higher soil evaporation rates contribute to rapid soil moisture loss at 100mm and 200mm, in contrast, shaded areas exhibit lower soil evaporation values. The transpiration rates are similar for both areas and are apparent at greater depths.

Changes in soil moisture at 600mm and 1000mm were likely linked to groundwater fluctuations, suggesting potential groundwater drawdown associated with hydrological drought. Prolonged dry conditions have been shown to contribute to groundwater depletion, as emphasized by Albers et al. (2015) and Ven et al. (2011). The results highlight the need to incorporate groundwater dynamics into urban drought assessments to enhance long-term drought predictions.

Root water uptake plays a significant role in soil moisture depletion, particularly in the upper soil layers. The study results demonstrate that during the drought, soil moisture at 100mm and 200mm declined rapidly across all measurement points, which can be attributed to root extraction by vegetation. The findings suggest that vegetation with shallow root systems is highly sensitive to drought conditions as soil moisture at these depths reached critically low levels before deeper layers were affected.

Interestingly, the study also indicated that initial soil moisture conditions influence root water uptake dynamics. In cases with initially wet conditions, the rate of moisture decline was steeper, suggesting that higher initial soil moisture conditions led to increased transpiration demand. However, over time, both wet and dry initial soil moisture conditions converged to similar moisture levels, reinforcing the idea that vegetation eventually depletes all available moisture within its root zone.

The deeper soil layers, 600mm and 1000mm, exhibit a delayed response to drought conditions visible in the measured and modelled soil moisture dynamics. This implies that deeper rooted vegetation may have access to more stable moisture reserves. However, the modeled soil moisture dynamics at these depths indicate a lack of significant moisture recovery, implying that restoring these values and improving groundwater levels requires more time than the modeled period allows. This finding underscores the long-term impact of drought on deep soil moisture availability and highlights the need for extended monitoring to fully capture groundwater recharge processes. Important to note is that the groundwater interactions are not modelled for this case and more research is needed for better knowledge about this process.

Soil texture plays a critical role in determining soil moisture retention, infiltration rates and overall drought resilience. The results of this study confirm that variations in soil texture significantly influenced moisture availability across different measurement points, becoming more important at increased depths. Measurement points with higher silt content, such as MP05, exhibited prolonged moisture retention compared to locations with higher sand content, such as MP01, which experienced rapid moisture depletion. This aligns with a study by N. Li et al. (2024) and Nelson and Miller (1997), indicating that finer-textured soils, such as silt and clay, have a higher water-holding capacity due to their smaller particle sizes and greater surface area, which enhances capillary forces.

Conversely, sandy soils drain more quickly, leading to lower moisture availability during drought conditions. The observed differences in soil moisture dynamics between these measurement points highlight the importance of considering soil composition when assessing urban drought impacts. Urban environments often feature a mix of compacted and distributed soil, which can further alter natural infiltration and retention patterns.

4.4. Limitations

While this study provides valuable insights into soil moisture dynamics during in urban areas, several limitations should be acknowledged.

First, the HYDRUS-1D model assumes only vertical flow and does not account for lateral redistribution. In urban environments, infrastructure and soil heterogeneity can significantly influence water movement, making lateral flow an important factor. Future studies should consider using HYDRUS-2D/3D to better capture these complex interactions.

Second, the model does not explicitly incorporate groundwater interactions, limiting its ability to simulate the hydrological drought effect accurately. The observed decline in deep soil moisture suggests groundwater drawdown, but without direct groundwater level measurements, this remains an assumption. Integrating groundwater data into future models would provide a clearer understanding of deep soil moisture dynamics.

Third, the study relies on soil moisture sensor data, which is subject to calibration errors. The generic calibration settings used in the sensor data might not fully capture site-specific soil characteristics, potentially leading to discrepancies between measured and modelled soil moisture values. Additionally, the determination of extreme initial soil moisture conditions in HYDRUS-1D was based on arbitrary adjustments to the measured soil moisture profile, which could have affected model convergence and water balance closure.

Finally, the study focuses on a single drought event, the drought of 2018, limiting the generalizability of the findings. While the results align with broader drought theories, analysing multiple drought events would provide a more comprehensive understanding of urban soil moisture responses under varying climatic conditions. Expanding the temporal scope of future studies would help determine whether the observed trends persist across different drought intensities.

5

Conclusion

This research aimed to identify the influence of urban environmental conditions on soil moisture dynamics during drought, with a particular focus on green spaces. By combining field measurements and numerical modeling using HYDRUS-1D, this research assessed how different urban environmental conditions, sun, shadow, grass, trees and paved areas, affected the soil-water balance. The findings emphasize the complex interactions between urban environmental conditions, soil texture and meteorological conditions, providing valuable insights which can be used in urban drought mitigation strategies. The conclusion is structured by the research questions.

How do urban environmental conditions affect soil moisture content in green spaces?
The results indicate that urban environmental conditions significantly influence soil moisture availability and variability. Sunny and shaded areas impact the transpiration and soil evaporation capacities of both grass and tree-covered locations. Shaded areas retained more soil moisture than sunny areas, primarily due to reduced evaporation rates.

Grass-covered areas showed the highest variability in soil moisture dynamics with rapid responses to precipitation events followed by gradual declines during dry periods. At greater depths, from 300mm and deeper (where grass roots are no longer present), the differences between sunny and shaded areas become more pronounced. Transpiration and evaporation rates were higher in areas with grass in sunny areas, while shaded areas contributed to prolonged soil moisture retention. Similar moisture dynamics were observed in shallow soil layers near trees, where the effects of shade from trees and buildings were comparable. However, determining the precise influence of trees on soil moisture remains challenging, as tree canopies intercept precipitation while extensive root systems affect soil water uptake and redistribution.

Paved areas exhibited the lowest soil moisture variability. The impervious surface prevented both infiltration and evaporation, resulting in consistently low soil moisture values. In addition to restricted infiltration, the sandy soil composition beneath paved surfaces further contributed to low moisture retention. These findings highlight the significant impact of urban design on soil-water balance and emphasize the importance of integrating permeable surfaces into city planning.

What is the effect of soil texture on soil moisture dynamics?
Soil texture was found to be a critical determinant of soil moisture retention and distribution, specifically at the deeper depths. The analysis of soil textures confirmed that finer-textured soils, such as silt- and clay-rich soils, exhibited higher water holding capacities compared to sand-dominated soils. Measurement points with a greater proportion of silt and clay retained moisture for longer periods, leading to slower depletion rates during dry conditions.

In contrast, sandy soils, characterized by larger pores and lower water holding capacity, drained more rapidly following precipitation events. These results align with previous studies that emphasize the role of soil texture in determining soil-water interactions. The study underscores the importance of considering soil properties in urban green space management, as areas with finer textured soils may require less frequent irrigation and provide greater resilience to drought stress.

How do initial soil moisture conditions influence soil moisture dynamics during a drought period, as modelled using HYDRUS-1D?
The HYDRUS-1D model effectively simulated the impact of the 2018 drought on soil moisture dynamics, for the grass-covered areas. The model successfully captured soil moisture fluctuations, although discrepancies were observed at greater depths due to interactions with groundwater.

The results indicate that initial soil moisture conditions can play a crucial role in soil water availability through a drought period. Wetter initial soil moisture resulted in prolonged moisture retention, maintaining higher soil moisture levels as the drought progressed. In contrast, drier initial soil moisture conditions led to a more rapid decline in soil moisture. However, the extremely wet initial soil moisture conditions have similar soil moisture values as the extremely dry initial conditions, at the end of the dry period.

These findings highlight the critical role of pre-drought soil moisture in shaping soil moisture dynamics. Wetter initial soil moisture conditions can buffer against more severe moisture depletion during prolonged droughts, in comparison to drier conditions, delaying the onset of critical moisture stress.

In conclusion, this study highlights the complex relationship between urban environmental conditions, soil texture and initial soil moisture conditions in shaping soil moisture dynamics during drought. The findings confirm that urban design significantly influences soil-water interactions, with vegetated and shaded areas enhancing moisture retention while paved surfaces worsen the soil dryness. Soil texture is a critical factor, particularly at greater depths where roots are no longer present anymore, where finer-textured soils provide better moisture and groundwater uplift, whereas sandy soils facilitate rapid drainage. Furthermore, the modeling results underscore the importance of initial soil moisture conditions, demonstrating that wetter starting conditions contribute to prolonged moisture availability during drought. These insights are valuable for urban drought mitigation strategies, emphasizing the need for green infrastructure, soil conscious urban planning, and proactive moisture management. Future research should further explore the complex effects of trees on soil moisture and integrate groundwater interactions to refine urban water balance models.

6 Recommendations

Based on the findings of this study, several recommendations can be made to improve the understanding of soil moisture dynamics in urban areas and enhance drought mitigation strategies. These recommendations focus on expanding the scope of future research, optimizing vegetation strategies, integrating findings into urban planning, and refining irrigation policies.

- **Expand study area and duration**
  This study was conducted on a small scale within a polder area over approximately 10 weeks. To develop a more comprehensive understanding of how urban environmental conditions influence soil moisture dynamics, future research should expand both the spatial and temporal scope of field measurements. Conducting long-term studies that encompass multiple dry periods, as defined by KNMI (2024), and extend across different urban areas would provide deeper insights into how soil moisture responds to varying climatic and infrastructural conditions. This would also allow for the inclusion of an actual drought period within the dataset, enabling validation of the dynamics observed in this study.

- **Vegetation**
  Vegetation type and root depth play a crucial role in transpiration and soil moisture retention. This suggests that plants with deeper root systems may have a stronger influence on soil moisture dynamics, especially at greater depths. Further studies should explore how different vegetation types, such as wildflowers increasingly introduced to enhance biodiversity, impact soil moisture retention and water distribution.

  Additionally, the effectiveness of native versus non-native plant species in mitigating urban drought should be assessed. While native plants may contribute to increased biodiversity, it remains unclear whether they support climate adaptation or exacerbate drought-related challenges. Similarly, tree species selection deserves further attention, as trees influence soil moisture not only through transpiration but also by interception and modifying evaporation rates. Understanding these effects more precisely would enable urban planners to select tree species that optimize soil moisture retention.

- **Urban planning**
  The results of the study highlight that urban design choices, such as the proportion of shaded versus sunny areas, the presence of impervious surfaces, and the soil composition in green spaces, significantly impact soil moisture levels. Therefore, urban planning strategies should incorporate soil-conscious design principles, ensuring that green spaces are developed with appropriate soil textures that enhance moisture retention. The use of finer soil textures, such as silt- and clay-rich soils (preferably a mixture of both textures), should be prioritized in green infrastructure projects, as these soil textures retain moisture more effectively than sandy soils.

  Additionally, urban development should integrate shading elements, such as strategically placed tree canopies or artificial structures, to reduce evaporation losses and promote long-term moisture retention. Permeable surfaces, such as water-absorbent pavements and rain gardens, should be implemented wherever possible to facilitate infiltration and mitigate excessive surface runoff. By incorporating these elements, future urban developments can be designed to be more resilient to prolonged dry periods.

- **Irrigation policies**
  Water management strategies must also evolve to address the importance of initial soil moisture conditions and the impact on the drought development. The findings suggest that maintaining higher soil moisture levels before the onset of a drought can slow moisture depletion rates, particularly in deeper soil layers. However, pre-drought irrigation policies should be carefully designed to balance benefits of moisture retention with the need for sustainable water usage.

  One potential strategy involves implementing urban drainage solutions, such as infiltration and drainage systems, which can supplement soil moisture by mimicking the role of groundwater recharge and ensuring a stable water supply at greater depths. Another approach could be to increase groundwater levels to enhance soil moisture content at increased depths. However, if irrigation is used, it is critical to adopt sustainable methods that do not compromise long-term water availability.

  It is important to note that pre-drought irrigation may reduce the soil's ability to absorb water during extreme rainfall events, potentially increasing flood risks. Therefore, careful planning and site-specific assessments are essential to avoid unintended consequences.

  Advancements in sensor-based irrigation technologies offer a promising solution for optimizing water distribution. Instead of relying on fixed irrigation schedules, smart irrigation systems can regulate water supply based on real-time soil moisture conditions. This approach prevents unnecessary water use while ensuring that vegetation remains resilient under drought stress. By integrating these strategies into urban water management, cities can enhance soil moisture retention while maintaining a sustainable balance between drought mitigation and flood prevention.

- **Model** Improvements in hydrological modelling approaches would further refine urban water management strategies. While HYDRUS-1D successfully simulated soil moisture fluctuations, some discrepancies were observed at greater depths due to interactions with groundwater. To enhance predictive accuracy, future research should consider adopting HYDRUS-2D or HYDRUS-3D, which would allow for a more comprehensive representation of the lateral water movement and interactions with urban infrastructure.

  Additionally, incorporating direct groundwater level measurements into future models would provide a more accurate representation of subsurface hydrological processes. Given the complexity of urban water flow dynamics, future models should also integrate the effects of urban infrastructure, such as underground utilities and drainage networks to better capture the interactions between built environments and soil moisture behaviour.

In summary, this study highlights the need for an integrated approach to urban drought mitigation, combining expanded research efforts, improved vegetation strategies, soil-conscious urban planning, sustainable irrigation policies, and enhanced hydrological modelling. By implementing these recommendations, cities can take the first measures in resilience to prolonged drought conditions, ensuring that urban green spaces remain viable and continue to provide environmental, social and economic benefits. Future research should focus on bridging the knowledge gaps regarding tree impacts, subsurface hydrology, and long-term urban soil moisture trends to further refine drought mitigation strategies and contribute to more climate adaptive environments.

References

Aboagye, P. D., & Sharifi, A. (2024, 1). Urban climate adaptation and mitigation action plans: A critical review. *Renewable and Sustainable Energy Reviews*, *189*. doi: 10.1016/j.rser.2023.113886

AHN. (2024). *AHN Viewer.* Retrieved from https://www.ahn.nl/ahn-viewer

Albers, R. A., Bosch, P. R., Blocken, B., van den Dobbelsteen, A. A., van Hove, L. W., Spit, T. J., … Rovers, V. (2015, 1). *Overview of challenges and achievements in the climate adaptation of cities and in the Climate Proof Cities program* (Vol. 83). Elsevier Ltd. doi: 10.1016/j.buildenv.2014.09.006

Allen, R. G., Pereira, L. S., Raes, D., & Smith, M. (1998). *Crop evapotranspiration - Guidelines for computing crop water requirements - FAO Irrigation and drainage paper 56*. Retrieved from https://www.fao.org/4/x0490e/x0490e00.htm#Contents

Bartholomeus, R. P., van der Wiel, K., van Loon, A. F., van Huijgevoort, M. H., van Vliet, M. T. H., Mens, M., … Pot, W. (2023, 5). Managing water across the flood-drought spectrum – experiences from and challenges for the Netherlands. *Cambridge Prisms: Water*, 1–22. doi: 10.1017/wat.2023.4

Bavel van, M., & Nichols, C. (2002). *Theta and Profiler Soil Moisture Probes - Accurate Impedance Measurement Devices - New Applications* (Tech. Rep.). Houston: Dynamax.

Berg, A., & Sheffield, J. (2018, 6). *Climate Change and Drought: the Soil Moisture Perspective* (Vol. 4) (No. 2). Springer. doi: 10.1007/s40641-018-0095-0

Bessembinder, J., Bintanja, R., Dorland, R. v., Homan, C., Overbeek, B., Selten, F., & Siegmund, P. (2023, 10). *KNMI'23-klimaatscenario's voor Nederland.* Retrieved from https://www.knmi.nl/kennis-en-datacentrum/achtergrond/knmi-23-klimaatscenario-s

Brown, P. W. (2000). *BASICS OF EVAPORATION AND EVAPOTRANSPIRATION Turf Irrigation Management Series: I* (Tech. Rep.). University of Arizona.

Bush, J., & Doyon, A. (2019, 12). Building urban resilience with nature-based solutions: How can urban planning contribute? *Cities*, *95*. doi: 10.1016/j.cities.2019.102483

Caiqiong, Y., & Jun, F. (2016, 4). Application of HYDRUS-1D model to provide antecedent soil water contents for analysis of runoff and soil erosion from a slope on the Loess Plateau. *Catena*, *139*, 1–8. doi: 10.1016/j.catena.2015.11.017

Calvin, K., Dasgupta, D., Krinner, G., Mukherji, A., Thorne, P. W., Trisos, C., … Ha, M. (2023, 7). *IPCC, 2023: Climate Change 2023: Synthesis Report, Summary for Policymakers. Contribution of Working Groups I, II and III to the Sixth Assessment Report of the Intergovernmental Panel on Climate Change [Core Writing Team, H. Lee and J. Romero (eds.)]. IPCC, Geneva, Switzerland.* (Tech. Rep.). IPCC. Retrieved from https://www.ipcc.ch/report/ar6/syr/ doi: 10.59327/IPCC/AR6-9789291691647.001

Chen, M., Willgoose, G. R., & Saco, P. M. (2014, 1). Spatial prediction of temporal soil moisture dynamics using HYDRUS-1D. *Hydrological Processes*, *28*(2), 171–185. doi: 10.1002/hyp.9518

Corovum Advies B.V. (2018, 3). *Module 6 - Riolering vD01.* Gouda.

Dabrowska, J., Menéndez Orellana, A. E., Kilian, W., Moryl, A., Cielecka, N., Michałowska, K., … Włóka, A. (2023, 11). *Between flood and drought: How cities are facing water surplus and scarcity* (Vol. 345). Academic Press. doi: 10.1016/j.jenvman.2023.118557

Daly, E., & Porporato, A. (2006, 6). Impact of hydroclimatic fluctuations on the soil water balance. *Water Resources Research*, *42*(6). doi: 10.1029/2005WR004606

Delta-T Devices Ltd. (2017). *User Manual for the Moisture Meter type HH2* (Tech. Rep.). Retrieved from http://www.delta-t.co.uk

FAO. (2006). *Soil Texture.* Retrieved from https://www.fao.org/fishery/static/FAO_Training/FAO_Training/General/x6706e/x6706e06.htm

Feddes, R. A., Kowalik, P., Kolinska-Malinka, K., & Zaradny, H. (1976, 9). Simulation of field water uptake by plants using a soil water dependent root extraction function. *Journal of Hydrology*, *31*(1-2), 13–26. doi: 10.1016/0022-1694(76)90017-2

Feddes, R. A., & Raats, P. A. C. (2004). *4 Parameterizing the soil-water-plant root system* (Tech. Rep.).

Wageningen: WUR.

Frank Lee. (2021). *Let me tell you 'bout the birds and the bees.* Retrieved from https://www.nk-tegelwippen.nl/waarom/

Heck, K., Coltman, E., Schneider, J., & Helmig, R. (2020, 10). Influence of Radiation on Evaporation Rates: A Numerical Analysis. *Water Resources Research*, *56*(10). doi: 10.1029/2020WR027332

Hoogheemraadschap Delfand. (2024, 10). *Het juiste waterpeil - Hoogheemraadschap van Delfland.* Retrieved from https://hhdelfland.maps.arcgis.com/apps/instant/sidebar/index.html?appid=b464f815c0af48178bdef923c11373e0

Jenerette, G. D., Harlan, S. L., Stefanov, W. L., & Martin, C. A. (2011, 10). Ecosystem services and urban heat riskscape moderation: water, green spaces, and social inequality in Phoenix, USA. *Ecological Applications*, *21*(7), 2637–2651. doi: 10.1890/10-1493.1

Jiang, W., Huang, Y., & Sha, A. (2018, 12). A review of eco-friendly functional road materials. *Construction and Building Materials*, *191*, 1082–1092. doi: 10.1016/j.conbuildmat.2018.10.082

Kabisch, N., Frantzeskaki, N., & Hansen, R. (2022, 6). Principles for urban nature-based solutions. *Ambio*, *51*(6), 1388–1401. doi: 10.1007/s13280-021-01685-w

Keyantash, J. (2021, 4). Springer Transactions in Civil and Environmental Engineering Hydrological Aspects of Climate Change. In A. Pandey, S. Kumar, & A. Kumar (Eds.), (chap. 11). Singapore: Springer.

Keyantash, J., & Dracup, J. A. (2002). *The Quantification of Drought: An Evaluation of Drought Indices* (Tech. Rep.).

KNMI. (2023). *Klimaatverandering.* Retrieved from https://www.knmi.nl/producten-en-diensten/klimaatverandering

KNMI. (2024, 10). *Neerslagtekort/Droogte.* Retrieved from https://www.knmi.nl/nederland-nu/klimatologie/geografische-overzichten/neerslagtekort_droogte

Kumar, P., Debele, S. E., Sahani, J., Rawat, N., Marti-Cardona, B., Alfieri, S. M., … Zieher, T. (2021, 8). *Nature-based solutions efficiency evaluation against natural hazards: Modelling methods, advantages and limitations* (Vol. 784). Elsevier B.V. doi: 10.1016/j.scitotenv.2021.147058

Learn Statistics Easily. (2024, 1). *Kendall Tau-b vs Spearman: Which Correlation Coefficient Wins?* Retrieved from https://statisticseasily.com/kendall-tau-b-vs-spearman/

Li, N., Skaggs, T. H., Ellegaard, P., Bernal, A., & Scudiero, E. (2024, 10). Relationships among soil moisture at various depths under diverse climate, land cover and soil texture. *Science of The Total Environment*, *947*, 174583. doi: 10.1016/j.scitotenv.2024.174583

Li, Z., Liu, H., Zhao, W., Yang, Q., Yang, R., & Liu, J. (2019, 11). Quantification of soil water balance components based on continuous soil moisture measurement and the Richards equation in an irrigated agricultural field of a desert oasis. *Hydrology and Earth System Sciences*, *23*(11), 4685–4706. doi: 10.5194/hess-23-4685-2019

Miralles, D. G., Brutsaert, W., Dolman, A. J., & Gash, J. H. (2022). On the use of the term 'Evapotranspiration'.
doi: 10.1002/essoar.10503229.1

Nabielek, K., & Hamers, D. (2015). *De stad verbeeld 12 infographics over de stedelijke leefomgeving* (Tech. Rep.). Den Haag.

Nalau, J., & Verrall, B. (2021, 1). Mapping the evolution and current trends in climate change adaptation science. *Climate Risk Management*, *32*. doi: 10.1016/j.crm.2021.100290

Nelson, J., & Miller, D. J. (1997). *Expansive soils: problems and practice in foundation and pavement engeneering*. New York: John Wiley & Sons.

Nguyen, G. N., Joshi, S., & Kant, S. (2017). Water availability and nitrogen use in plants: effects, interaction, and underlying molecular mechanisms. In *Plant macronutrient use efficiency* (pp. 233–243). Elsevier. doi: 10.1016/B978-0-12-811308-0.00013-2

Ouédraogo, A. A., Berthier, E., Sage, J., & Gromaire, M.-C. (2025, 2). Modelling evapotranspiration in urban green stormwater infrastructures: Importance of sensitivity analysis and calibration strategies with a hydrological model. *Environmental Modelling & Software*, *185*, 106319. Retrieved from https://linkinghub.elsevier.com/retrieve/pii/S1364815225000039 doi: 10.1016/j.envsoft.2025.106319

Paudel, S., & States, S. L. (2023, 6). *Urban green spaces and sustainability: Exploring the ecosystem services and disservices of grassy lawns versus floral meadows* (Vol. 84). Elsevier GmbH. doi:

10.1016/j.ufug.2023.127932

PC -Progress. (2021). *HYDRUS.* Retrieved from `https://www.pc-progress.com/en/Default.aspx?hydrus`

Peters, E. B., Hiller, R. V., & McFadden, J. P. (2011, 3). Seasonal contributions of vegetation types to suburban evapotranspiration. *Journal of Geophysical Research: Biogeosciences*, *116*(1). doi: 10.1029/2010JG001463

Puth, M. T., Neuhäuser, M., & Ruxton, G. D. (2015, 4). *Effective use of Spearman's and Kendall's correlation coefficients forassociation between two measured traits* (Vol. 102). Academic Press. doi: 10.1016/j.anbehav.2015.01.010

Rabot, E., Wiesmeier, M., Schlüter, S., & Vogel, H. J. (2018, 3). *Soil structure as an indicator of soil functions: A review* (Vol. 314). Elsevier B.V. doi: 10.1016/j.geoderma.2017.11.009

Rana, G., & Katerji, N. (2000). *Measurement and estimation of actual evapotranspiration in the field under Mediterranean climate: a review* (Vol. 13; Tech. Rep.). Retrieved from `www.elsevier.com/locate/eja`

Richards, L. A. (1931, 11). CAPILLARY CONDUCTION OF LIQUIDS THROUGH POROUS MEDIUMS. *Physics*, *1*(5), 318–333. doi: 10.1063/1.1745010

Rijksoverheid. (2023, 3). *Inhoudelijke maatlat: op hoofdlijnen* (Tech. Rep.). Retrieved from `https://www.rijksoverheid.nl/documenten/kamerstukken/2021/09/21/bijlage-op-weg-naar-`

Rijkswaterstaat. (2019). *Bescherming tegen droogte.* Retrieved from `https://www.rijkswaterstaat.nl/water/waterbeheer/bescherming-tegen-het-water`

Rijkswaterstaat. (2022). *Droogte en Watertekort in Nederland.* Retrieved from `https://www.rijkswaterstaat.nl/water/waterbeheer/droogte-en-watertekort`

Šimůnek, J., Van Genuchten, M. T., & Šejna, M. (2012). *The HYDRUS Software Package for Simulating the Two-and Three-Dimensional Movement of Water, Heat, and Multiple Solutes in Variably-Saturated Porous Media Technical Manual Version 2.0* (Tech. Rep.).

Steudle, E., & Peterson, C. A. (1998, 5). How does water get through roots? *Journal of Experimental Botany*, *49*(322), 775–788. doi: 10.1093/jxb/49.322.775

Tanaka, K., & Hashimoto, S. (2006, 7). Plant canopy effects on soil thermal and hydrological properties and soil respiration. *Ecological Modelling*, *196*(1-2), 32–44. doi: 10.1016/j.ecolmodel.2006.01.004

UNFCC. (2016). *The Paris Agreement.* Retrieved from `https://unfccc.int/process-and-meetings/the-paris-agreement`

United Nations. (2016, 4). *List of parties that signed the Paris Agreement on 22 April.* Retrieved from `https://www.un.org/sustainabledevelopment/blog/2016/04/parisagreementsingatures/`

Valentine, E. M., & Apelt, C. J. (2011). *Proceedings of the 34th World Congress of the International Association for Hydro-Environment Research and Engineering : 33rd Hydrology and Water Resources Symposium and 10th Conference on Hydraulics in Water Engineering*. Engineers Australia.

Ven, F. v. d., Nieuwkerk, E. v., Stone, K., Veerbeek, W., Rijke, J., Herk, S. v., & Zevenbergen, C. (2011). *Building the Netherlands climate proof: urban areas*.

Vorwerk, S., Cameron, D., & Keppel, G. (2015). Clay Soil in Suburban Environments. In *Ground improvement case histories* (pp. 655–682). Elsevier. doi: 10.1016/B978-0-08-100191-2.00022-8

Wang, J.-W., Yang, H.-J., & Kim, J.-J. (2020, 10). Wind speed estimation in urban areas based on the relationships between background wind speeds and morphological parameters. *Journal of Wind Engineering and Industrial Aerodynamics*, *205*, 104324. doi: 10.1016/j.jweia.2020.104324

Xiao, C., Ye, J., Esteves, R. M., & Rong, C. (2016, 9). Using Spearman's correlation coefficients for exploratory data analysis on big dataset. *Concurrency and Computation: Practice and Experience*, *28*(14), 3866–3878. doi: 10.1002/cpe.3745

Yimer, E. A., De Trift, L., Lobkowicz, I., Villani, L., Nossent, J., & van Griensven, A. (2024, 2). *The underexposed nature-based solutions: A critical state-of-art review on drought mitigation* (Vol. 352). Academic Press. doi: 10.1016/j.jenvman.2023.119903

Zhang, B., Xie, G.-d., Gao, J.-x., & Yang, Y. (2014, 6). The cooling effect of urban green spaces as a contribution to energy-saving and emission-reduction: A case study in Beijing, China. *Building and Environment*, *76*, 37–43. doi: 10.1016/j.buildenv.2014.03.003

Zhang, X., Chen, N., Sheng, H., Ip, C., Yang, L., Chen, Y., … Niyogi, D. (2019, 11). *Urban drought challenge to 2030 sustainable development goals* (Vol. 693). Elsevier B.V. doi: 10.1016/j.scitotenv.2019.07.342

Zhang, Y., Van den Berg, A. E., Van Dijk, T., & Weitkamp, G. (2017, 5). Quality over Quantity: Contribution of Urban Green Space to Neighborhood Satisfaction. *International journal of environmental research and public health*, *14*(5). doi: 10.3390/ijerph14050535

A

Measurement procedure

The measurement procedure is outlined below. Each measurement follows these steps: Setting Up the Measuring Device (HH2 Moisture Meter)

1. Connect the battery at the back.
2. Turn on the device by pressing `Esc`.
3. Press `Set` to enter the menu (use the arrow keys to navigate).
   (a) Select *Soil type* and press `Set`.
   (b) Select *All sensors* and press `Set`.
   (c) Select *Organic/Mineral* and press `Set`.
4. Press `Read` to take a measurement.
5. Write down the sensor reading in the spreadsheet
6. Rotate the sensor by 1/3 and repeat the measurement.
7. Take three measurements per measurement point.
8. At the end of the measurements, disconnect the battery.

Table A.1: The measurement points and belonging soil type setting on the HH2 Moisture Meter

MP	**Soil type**
MP01	Organic
MP02	Organic
MP03	Organic
MP04	Mineral
MP05	Mineral
MP06	Mineral
MP07	Mineral
MP08	Organic
MP09	Organic
MP10	Organic

B
Measurement results

The soil moisture data per measurement point is depicted below. Each measurement point is measured at five depths, 100mm, 200mm, 300mm, 600mm and 1000mm. The measurement point number and belonging description are in Table 2.1.

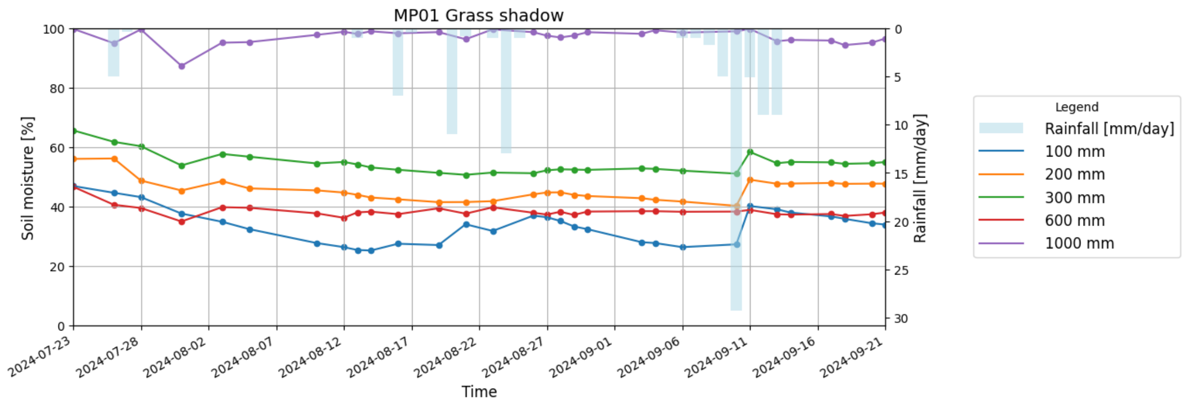

(a) MP01

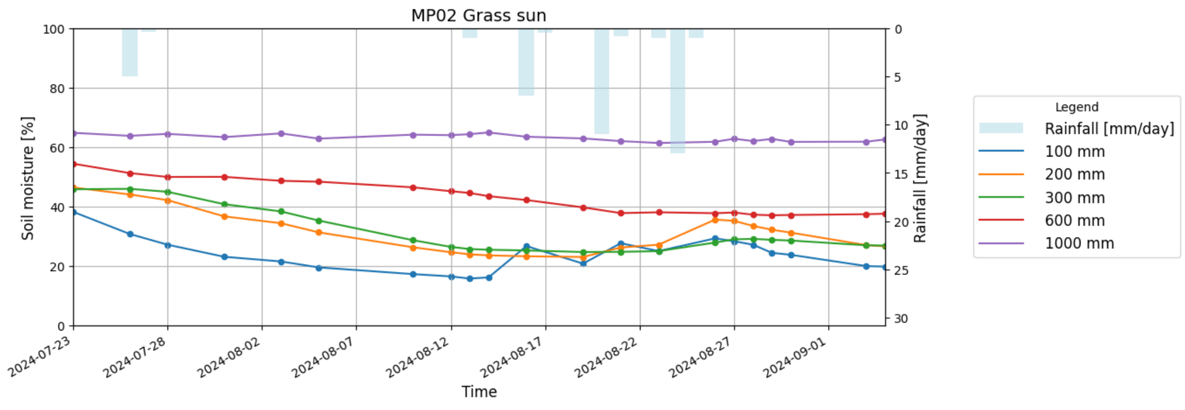

(b) MP02

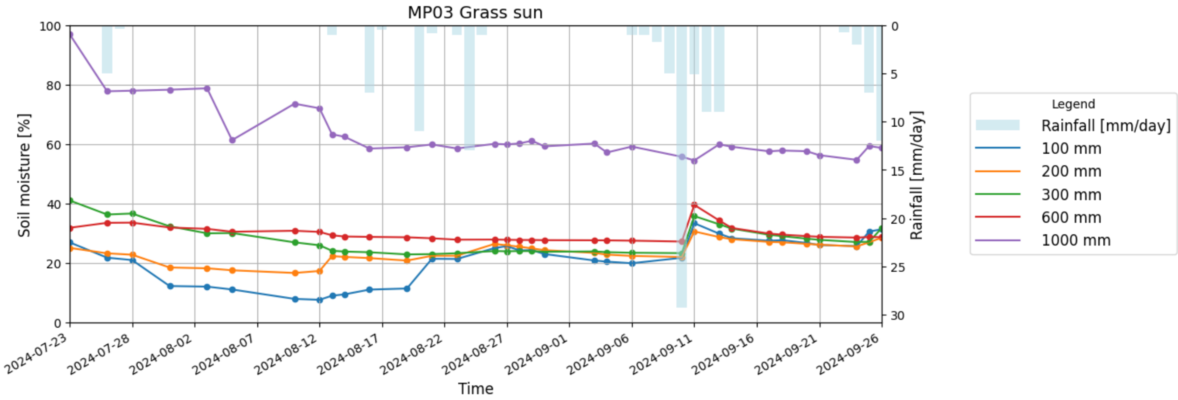

(c) MP03

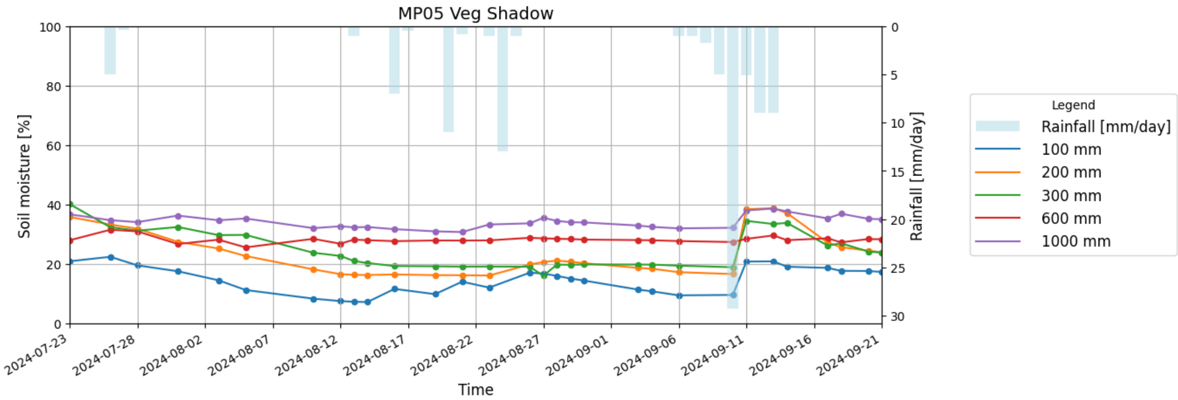

(d) MP05

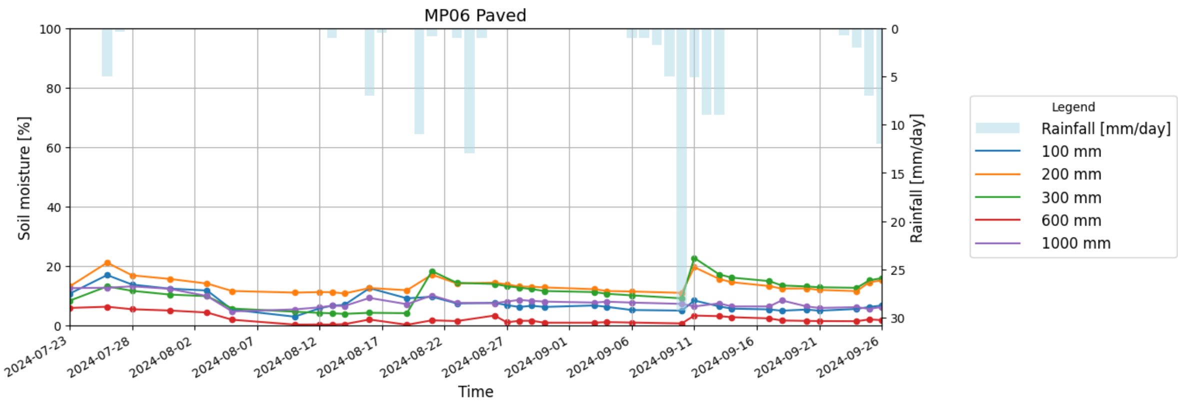

(e) MP06

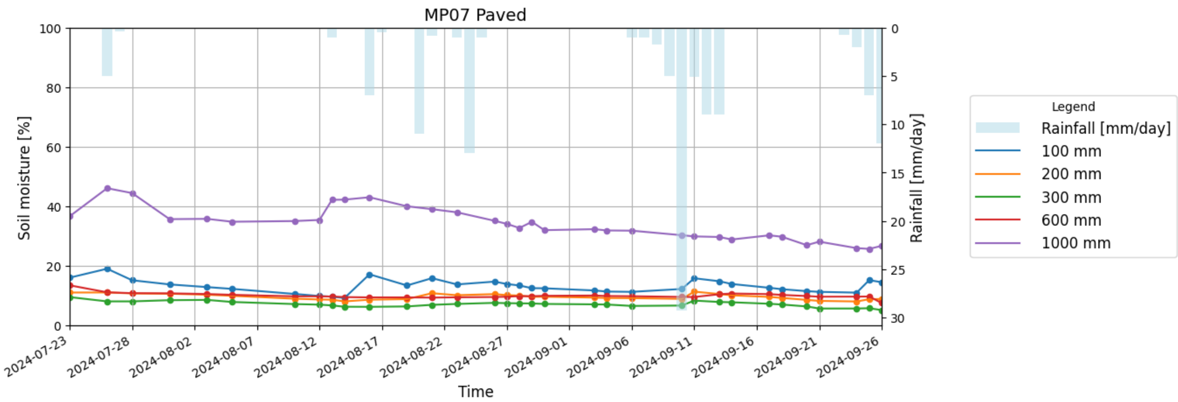

(f) MP07

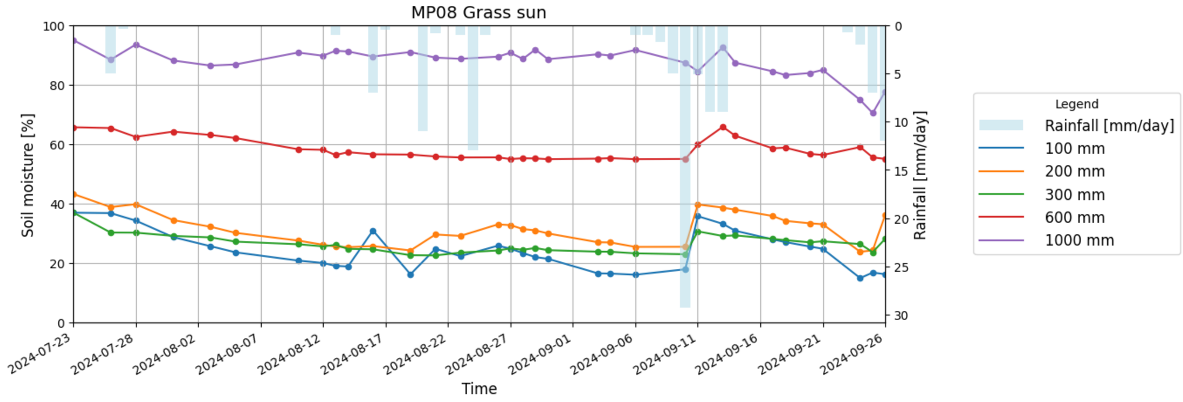

(g) MP08

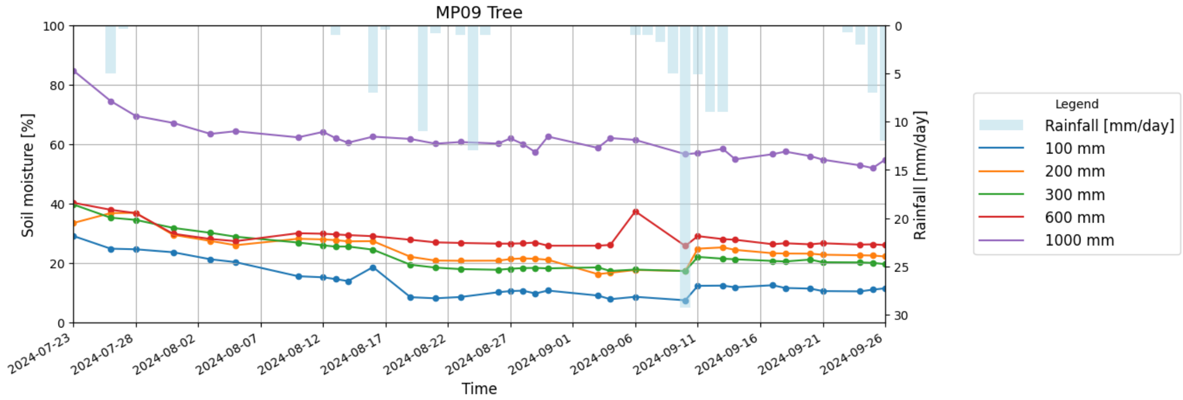

(h) MP09

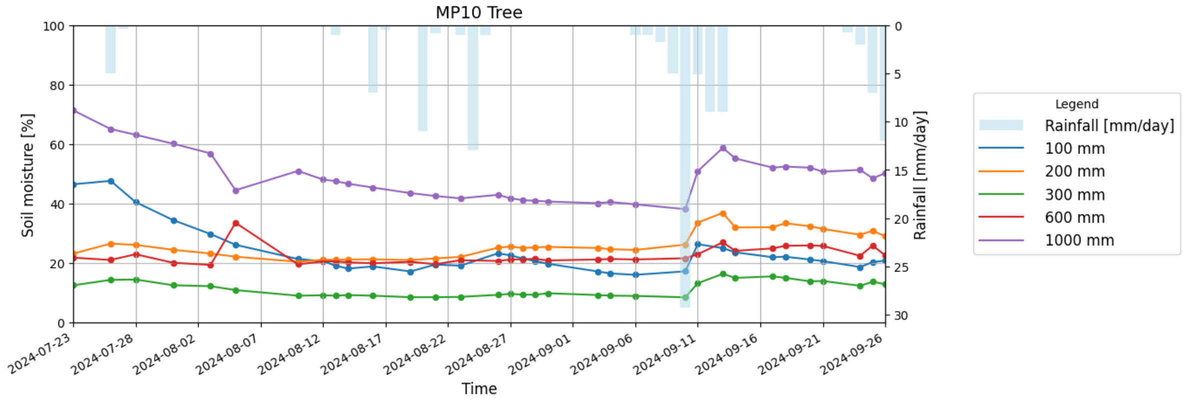

(i) MP10

Figure B.1: Soil moisture dynamics of all measurement points categorized by measurement point.